JOURNAL OF GEOPHYSICAL RESEARCH, VOL. 105, NO. B9, PAGES 21,559–21,578, SEPTEMBER 10, 2000

Anomalous splitting of free oscillations: A reevaluation of possible interpretations

Barbara Romanowicz and Ludovic Bréger

Seismological Laboratory, University of California, Berkeley

Abstract. The splitting of normal modes sensitive to structure in the inner core is larger than can be explained by three-dimensional heterogeneity confined to the earth's mantle. A preferred interpretation of this anomalous splitting involves inner core anisotropy, providing a unified explanation of these data and of observed trends in the travel times of PKP waves that sample the inner core. We reexamine this interpretation, as well as a previously suggested alternative one in terms of outer core structure. Our motivation comes from recent results which indicate that simple, smooth models of inner core anisotropy are in disagreement with some PKP observations. We invert a recently assembled high quality dataset, comprising modes sensitive to mantle and outermost core structure, as well as modes sensitive to mantle, outer core and inner core structure. We compare models parametrized to include either inner core anisotropy or heterogeneity in the outer core. We show the following: (1) Outer core models, with fewer parameters, provide good overall fits to most modes with weak or strong sensitivity in the inner core, except for mode ${}_3S_2$, the inner core mode with the strongest splitting. (2) V_s and ρ profiles obtained for models with outer core structure using mantle and core modes are in better agreement with those obtained using data sensitive to mantle structure alone, whereas the V_p structure in D" shows a stronger c_{20} component when inner core anisotropy is considered. (3) Lateral heterogeneity restricted to the mantle, in particular strong heterogeneity in D", fails to account consistently for the splitting of all modes. Outer core models thus deserve further investigation and should be weighted against more complex models of inner core anisotropy to explain anomalous splitting of normal modes and PKP travel times. The outer core structure obtained, while arguably unrealistic, is consistent with concentration of light elements, either confined to the Taylor cylinder tangent to the inner core or in polar caps at the top and bottom of the outer core. A small amount of shear within such polar caps might account for the excess splitting of some core modes.

1. Introduction

Inner core anisotropy was proposed 15 years ago to explain two categories of intriguing observations: (1) faster propagation times for seismic body waves that travel through the inner core along paths quasi-parallel to the Earth's rotation axis than for those that travel on equatorial paths [*Poupinet et al.*, 1983; *Morelli et al.*, 1986], and (2) anomalous splitting of core-sensitive free oscillations [*Masters and Gilbert*, 1981; *Woodhouse et al.*, 1986]. These observations have been confirmed in many subsequent studies [*e.g., Shearer et al.*, 1988; *Shearer*, 1991; *Creager*, 1992; *Vinnik et al.*, 1994; *Su and Dziewonski*, 1995; *Song*, 1996] and models of inner core anisotropy have been progressively refined. These models were originally cast in terms of constant transverse isotropy with fast axis parallel to the Earth's rotation axis, for which an interpretation in terms of alignment of hcp-Fe crystals was proposed. Such an interpretation was later reinforced by theoretical computations [*Stixrude and Cohen*, 1995]. Over the years, inner core anisotropy models have become more complicated. Depth dependence was introduced [*Su and Dziewonski*, 1995; *Tromp*, 1993] and a more complex spatial distribution was suggested [*Li et al.*, 1991; *Romanowicz et al.*, 1996; *Durek and Romanowicz*, 1999]. Most recently, several studies have proposed even stronger departures from simple models of inner core anisotropy. An asymmetry in the anisotropy pattern was pointed out [*Tanaka and Hamaguchi*, 1997; *Creager*, 1999], with one "quasi-hemisphere" of the inner core anisotropic and the other not, and it has been argued that the top 100-200 km of the inner core may be isotropic and laterally varying [*Song and Helmberger*, 1998]. Strong,

Paper number 2000JB900144.
0148-0227/00/2000JB900144$09.00

small-scale variations in the anisotropy along a highly anomalous path between the South Sandwich Islands and station COL in Alaska have also been documented [*Creager,* 1997].

The necessity to modify the simple original model of constant anisotropy and to introduce significant complexity has become quite clear. Moreover, we have recently proposed that an important contribution to the trend of travel time residuals, as a function of angle of the path with respect to the rotation axis, for $PKP(AB) - PKP(DF)$ data, could come from strong heterogeneity in D" [*Bréger et al.,* 2000], and we suggested a possible trade-off between D" structure and inner core anisotropy in the interpretation of differential PKP travel time data. Also, we have shown that global $PKP(BC) - PKP(DF)$ data require very short scale lateral variations in the inner core anisotropy, which, again, could alternatively be interpreted in terms of contributions of strong heterogeneity in D" [*Bréger et al.,* 1999], causing large excursions with respect to an average constant inner core anisotropy model with a maximum strength of ~1.5%.

Even if we accept an interpretation of PKP data in terms of a complex inner core anisotropy model, some of the recent observations need to be reconciled with the normal mode splitting data. Indeed, since normal modes are primarily sensitive to even order structure, it is difficult to reconcile the hemispherical model [*Tanaka and Hamaguchi,* 1997; *Creager,* 1999] with the dominant zonal "c_2^0" component of anomalous splitting observations. Likewise, since modes with the largest splitting are primarily sensitive to the uppermost third of the inner core, their splitting becomes more difficult to explain in terms of anisotropy if there is an isotropic layer, several hundred kilometers thick, at the top of the inner core [*Durek and Romanowicz,* 1999].

Alternative interpretations for anomalous mode splitting have been proposed in terms of outer core heterogeneity [*Ritzwoller et al.,* 1986; *Widmer et al.,* 1992]. In particular, they have shown that inner core anisotropy models tend to overpredict the splitting of modes that have large energy in the inner core and to underpredict that of modes that have little (i.e., < 4%) energy there. However, depth dependence of anisotropy can account for some of these effects [*Tromp,* 1995], and in any case, the outer core interpretation has not received further attention, because "realistic" models require significant levels of heterogeneity in density in the outer core, and these are thought to be ruled out from dynamic considerations [*Stevenson,* 1987]. Alternatively, if density is kept at its presumed hydrostatic level, the velocity model inferred implies very unusual relations between elastic parameters in the outer core [*Widmer et al.,* 1992].

In view of the recent controversies regarding the level and complexity of inner core anisotropy, it is desirable to reexamine the interpretation of anomalous mode splitting data. We are assisted in this process by the recent accumulation of high-quality low-frequency data, owing to the expansion of the global digital broadband network and the occurrence of several very large deep earthquakes, among them the $M8.2$ Bolivia earthquake of June 9, 1994.

Previous authors have inverted core-sensitive mode data for core structure, after correcting for mantle structure using available tomographic models of the mantle. A key element of our study is that we invert simultaneously for mantle and core structure using both mantle and core mode data, arguing that (1) the combined data set increases the resolution of structure in the mantle; (2) it is important that the structure obtained be compatible with all mantle and core mode data; and (3) correcting for mantle structure generally requires to introduce strong a priori assumptions on the relative variations of V_s, V_p and ρ, which we wish to avoid.

2. Data Analysis

We have assembled a splitting data set for 83 spheroidal normal modes sensitive either to structure in the mantle and outer core (60 modes) or to structure in the mantle, outer core and inner core (23 modes). These data are tabulated in terms of measured splitting coefficients, as defined below, from three sources: measurements by *Resovsky and Ritzwoller* [1998] mostly for mantle modes, by *He and Tromp* [1996] for a combination of mantle and core modes, complemented by our own dataset, primarily for core modes [*Durek and Romanowicz,* 1999], as well as a dataset of 31 toroidal modes [*Tromp and Zanzerkia,* 1995; *Resovsky and Ritzwoller,* 1998]. We have excluded from this dataset several spheroidal modes for which the measurements are suspicious because they differ significantly from author to author and/or from any reasonable predictions. These modes are ${}_1S_{14}$, ${}_3S_7$, ${}_3S_8$ and ${}_{17}S_1$.

Splitting coefficients (c_s^t) were introduced by Woodhouse et al. (1986) as a convenient way to represent the splitting of normal modes. They are coefficients of a spherical harmonics expansion on the unit sphere of a function $c(\theta, \phi)$, which, much as phase velocity maps for surface waves, represents effects of structure and anisotropy on a particular mode, integrated over depth below each point (θ, ϕ):

$$c(\theta, \phi) = \sum_{s,t} c_s^t Y_s^t(\theta, \phi) \tag{1}$$

$$c_s^t = \sum_i \int_0^a \delta m_{st}^i(r) M_s^i(r) dr + \sum_d \delta h_{st}^d H_s^d, \tag{2}$$

where $\delta m_{st}(r)$ are coefficients of spherical harmonics expansions of perturbations in S velocity (V_s), P velocity (V_p), density (ρ) and/or anisotropic parameters (index i), δh_{st}^d represent topography of discontinuities d, and the corresponding kernels $M_s^i(r)$, and H_s^d are given by *Li et al.* [1991].

The anomalous splitting detected in core modes has been shown to affect predominantly the zonal c_2^0 coefficient. A small set of modes also exhibit anomalous c_4^0, but this coefficient is much more poorly constrained. Although we also invert for c_4^0, as well as the radially symmetric perturbation c_0^0, we will not discuss the results here, but rather we focus on degree 2 coefficients and particularly c_2^0, since other large coefficients such as c_2^2 and s_2^2 can be largely explained by mantle structure alone, even for inner core sensitive modes. The observations, as provided by the respective authors, have been corrected for the effect of rotation and hydrostatic ellipticity.

Figures 1a and 1b show a comparison of data for spheroidal modes from the three sources considered, giving a sense of uncertainty on the splitting measurements. In most cases, agreement between different groups are excellent (also with measurements from G. Laske and G. Masters (personal communication,1999)). We have distinguished mantle modes (Figure 1a) and modes with sensitivity to inner-core structure (Figure 1b). We classify the latter into two categories: (1) those with $< 4\%$ sensitivity to inner core structure (modes ${}_1S_2$-${}_{21}S_8$, category "ic1") and (2) those with stronger sensitivity to inner core structure (modes ${}_8S_1$-${}_3S_2$, category "ic2"). Mode ${}_3S_2$ has been assigned to category ic2, only because it has significant sensitivity to S-velocity in the inner core. We will single out this particular mode, which exhibits the strongest anomalous splitting, the largest uncertainties in the measurements, as well as the largest sensitivity to inner core anisotropy. We have also plotted the splitting predictions of mantle model SAW12D [*Li and Romanowicz,* 1996)], an *SH* model of the mantle, obtained using body and surface waveform data. In order to compute splitting predictions we have assumed standard conversion factors: $\mathrm{d}\ln V_p/\ \mathrm{d}\ln V_s$=0.5 and $\mathrm{d}\ln\rho/\mathrm{d}\ln V_s$=0.25, as proposed by *Li et al.* [1991]. Predictions for other mantle models are similar. Two observations are striking: for mantle modes the predictions of SAW12D follow the data quite closely for all branches, although the amplitudes in the ${}_0S$ and ${}_2S$ branches are underpredicted. For inner core sensitive modes, we note, as did previous authors, that the mantle model predicts practically no splitting, whereas the data consistently show a high level of splitting. This is referred to, in the literature, as "anomalous" splitting. We note that except for mode ${}_3S_2$, the level of splitting observed for modes in categories ic1 and ic2 is comparable, with a few modes exhibiting somewhat larger splitting in both data sets (${}_2S_3$ and ${}_6S_3$ in ic1 and ${}_{13}S_1$, ${}_{13}S_2$ in ic2). In Figure 1c we show the corresponding toroidal mode data [*Tromp and Zanzerkia,* 1995; *Resovsky and Ritzwoller,* 1998]. We note that the scatter is here much larger than for spheroidal mode data around the theoretical predictions of model SAW12D. Therefore we have chosen to include only measurements of *Resovsky*

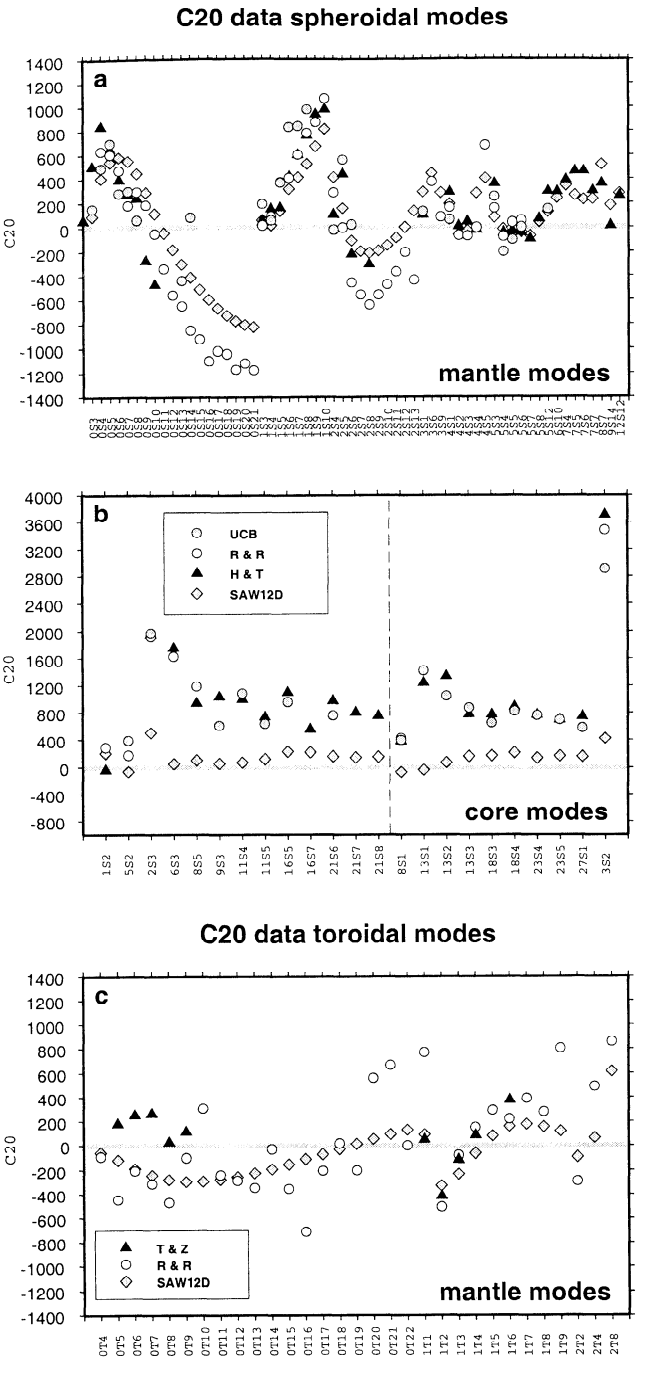

Figure 1. The c_2^0 splitting data for (a,b) spheroidal modes and (c) toroidal modes, expressed relative to the PREM center frequency in units of 10^{-6} [cf. He and Tromp, 1996]. UCB, data from *Durek and Romanowicz* [1999]; R&R, from *Resovsky and Ritzwoller* [1998]; H&T, from *He and Tromp* [1996]. T&Z, from *Tromp and Zanzerkia* [1995]. Figure 1a shows mantle and outer core modes and Figure 1b shows inner core sensitive modes. Note the change of scale on the vertical axis in Figure 1b. The core modes have been subdivided (vertical dashed line) into those that have small sensitivity to inner core structure (${}_1S_2$-${}_{21}S_8$) and those that have more than 4% of their energy in the inner core (${}_8S_1$-${}_3S_2$). Also shown are the predictions of SAW12D, a mantle model derived from *SH* waveform data [*Li and Romanowicz,* 1996].

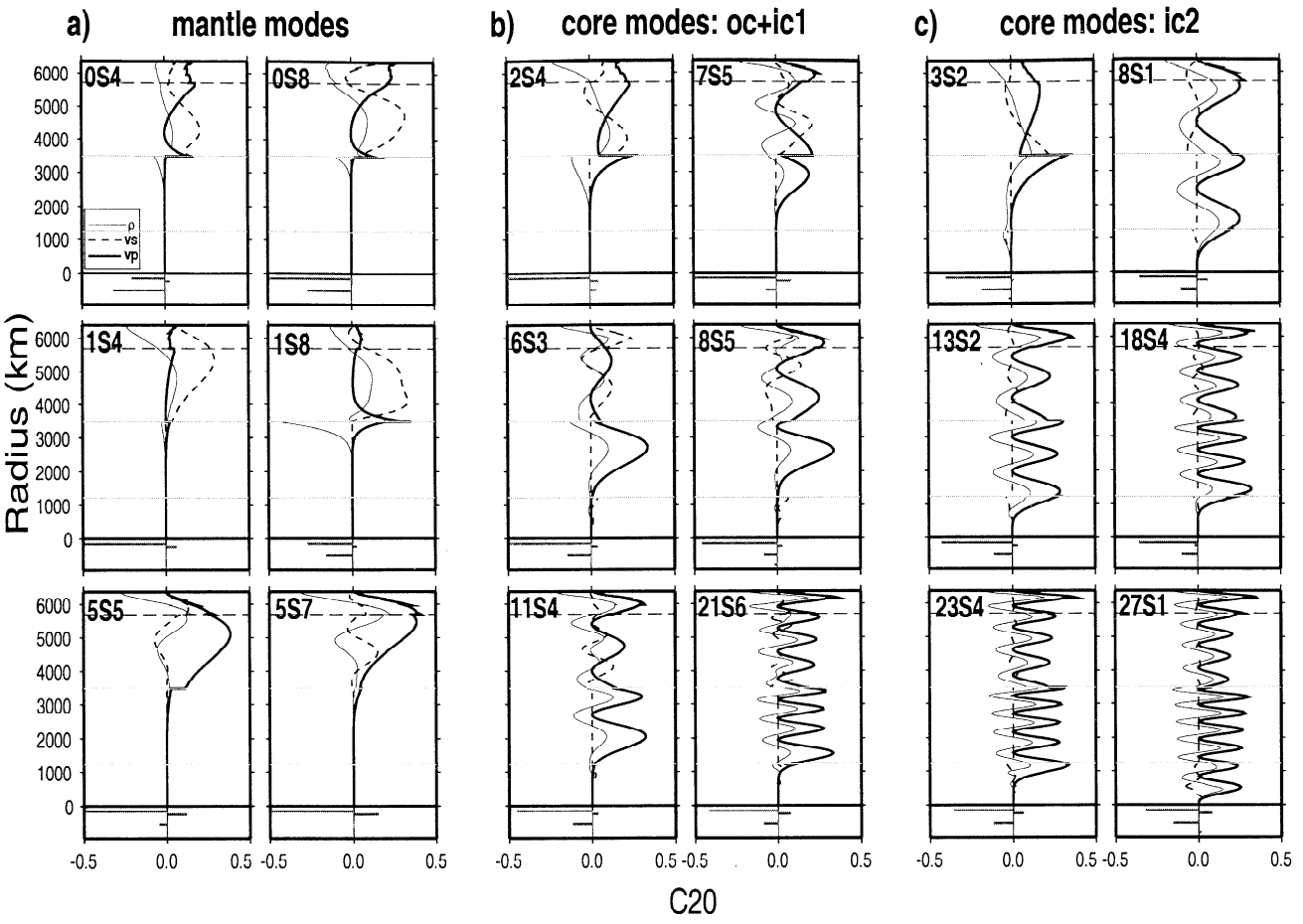

Figure 2. Sensitivity kernels in c_2^0 for representative modes. (a) Mantle modes, (b) outer core modes ("oc") and modes with little sensitivity to inner core ("ic1") and (c) modes with significant energy in the inner core ("ic2"). At the bottom of cach plot, the sensitivity to topography is given for the following discontinuities, from top to bottom: Moho, 670 km, core-mantle boundary (CMB), inner core boundary.

and Ritzwoller [1998] for modes ${}_0T_6$-${}_0T_8$, ${}_0T_{12}$-${}_0T_{14}$, ${}_1T_2$-${}_1T_8$, and ${}_2T_2$, ${}_2T_4$, ${}_2T_8$ in our inversions, as the observations are the most compatible with the predictions of the SH model SAW12D. We will show that inclusion of toroidal modes has no significant effect on our conclusions. On the other hand, we have kept all the data displayed in Figures 1a and 1b except mantle modes with particularly large excursions from smooth variations with angular order along a given branch (e.g., ${}_4S_5$, ${}_2S_{13}$). We have kept the measurements of *Resovsky and Ritzwoller* [1998] for most mantle modes, except ${}_0S_3$-${}_0S_6$, for which we keep the Berkeley measurements, and all modes on the right of ${}_5S_4$, for which we keep the *He and Tromp* [1996] measurements. For spheroidal core modes we have used our own measurements for modes for which they exist and *He and Tromp*'s [1996] otherwise. As we have verified, modifying the choice of c_2^0 values for a few modes does not affect our conclusions.

Figure 2 shows examples of sensitivity kernels for the c_2^0 splitting coefficient as a function of depth computed with respect to the radially symmetric model PREM [*Dziewonski and Anderson,* 1981]. Note that the core modes (Figures 2b and 2c) also have significant sensitivity to mantle structure, in particular, in V_p and ρ.

We invert these data using the following parametrization. We consider simple layered models of V_s, V_p, and ρ in the mantle (Table 1), V_p and ρ in the outer core and models of inner core anisotropy with various levels of complexity, as allowed by the axisymmetric formalism developed by Li et al. (1991) and applied more recently to broadband data [*Romanowicz et al.*, 1996; *Durek and Romanowicz,* 1999]. We also include topography on two discontinuities (670-km discontinuity, and core-mantle boundary (CMB)). We will discuss the effect of including topography of the CMB in section 4.

In order to better assess where the inversions naturally tend to put the structure, we apply no other smoothness constraints than overall damping, represented by a single damping parameter, the reference model being spherically symmetric [PREM, *Dziewonski and Anderson,* 1981]. All modes are given equal weighting in the inversion. After some experimenta-

Table 1. Mantle Model Parametrization

Layer Depths, km	Index
33-250	1
250-450	1
450-670	1
670-1000	3
1000-1300	3
1300-1500	3
1500-1700	3
1700-1900	3
1900-2100	3
2100-2300	3
2300-2500	3
2500-2700	3
2700-2891	3

Discontinuities are Moho, 670 km and CMB. Index is 1 if $dV_p/V_p = 0.5dV_s/V_s$, and $d\rho/\rho = 0.25dV_s/V_s$, and index is 3 if V_p, V_s, and ρ are solved for independently.

tion, we have arrived at a layered parametrization which yields stable and relatively smooth models using mantle modes (Table 1, three layers in the crust/upper mantle, ten layers in the lower mantle). For most of the cases discussed here, we invert for V_s only in the upper mantle and down to 1300 km depth, assuming V_p and ρ to be proportional to V_s, consistent with findings of independent studies based on normal modes and travel times [*Robertson and Woodhouse,* 1995; *Su and Dziewonski,* 1997; *Ishii and Tromp,* 1999; *Kuo et al.*, 1998]. Below 1600 km, we solve separately for V_s, V_p and ρ. Previous studies have shown that the proportionality between V_p and V_s may break down below a depth of 1800-2000 km, which may result in different depth profiles for c_2^0 in V_s, V_p and ρ respectively [*Robertson and Woodhouse,* 1995, 1996; *Bolton and Masters,* 1996; *Kuo et al.,* 1998]. Whether or not we impose a proportionality constraint in the lower mantle has no incidence on our conclusions regarding the core, as we show in section 4.

In the outer core we consider one or several layers and solve for V_p and ρ without any a priori constraints on the ρ structure. Several one layer models are considered, with increasing thickness, starting from the top (or the bottom) of the outer core.

Three parametrizations of inner core anisotropy are considered: (1) a simple constant transverse anisotropy model (three independent variables, "i1 models"), (2) a model of transverse anisotropy with depth dependence, described by a polynomial in r^2 up to degree 4 (15 independent variables, "i2 models"), and (3) a more general axisymmetric model including lateral variations expressed in spherical harmonics up to degree 4 (44 independent parameters, "i3 models"). The nomenclature of models is summarized in Table 2. Note also that for models with heterogeneity in the mantle and outer core, inversions of c_2^0 and c_4^0 are independent. For models that include inner core anisotropy, on the other hand,

Table 2. Nomenclature of Models Considered in This Study.

Model Index	Mantle	Outer Core	Inner Core	Number of Parameters in the Core
a	yes	no	no	0
b	yes	1 layer: 2891-3200 km	no	2
c	yes	1 layer: 2891-3500 km	no	2
d	yes	1 layer: 2891-4000 km	no	2
e	yes	1 layer: 2891-4500 km	no	2
f	yes	1 layer: 2891-5100 km	no	2
u	yes	4 layers: 2891-3500 km 3500-4000 km 4000-4500 km 4500-5100 km	no	8
v	yes	6 layers: 2891-3191 km 3191-3491 km 3491-3891 km 3891-4291 km 4291-4691 km 4691-5150 km	no	12
x	yes	1 layer: 3500-5100 km	no	2
y	yes	1 layer: 4000-5100 km	no	2
z	yes	1 layer: 4500-5100 km	no	2
i1	yes	no	anisotropy[a]	3
i2	yes	no	anisotropy[b]	15
i3	yes	no	anisotropy[c]	44

[a]Constant transverse isotropy.
[b]Depth dependent transverse isotropy.
[c]General axisymmetric anisotropy.

Table 3. Indexing of Subsets of Modes Used in the Inversions

Index	Mode Subset
1	mantle and outer core modes only
2	mantle, outer core and ic1 modes
3	mantle, outer core and ic2 modes, without ${}_3S_2$
4	mantle, outer core and ic2 modes, with ${}_3S_2$
5	all modes without ${}_3S_2$
6,7,8,9	all modes with ${}_3S_2$

they are coupled. On the whole, we will show results of inversions for 12 different depth parametrizations.

In what follows, we present the results of inversions performed using different subsets of data. Mantle and outer core (oc) modes are always included, and we distinguish four main families of inversions: (1) mantle and outer core modes only; (2) ic1 modes included; (3) ic2 modes included; and (4) all modes included. In the latter two cases, we also distinguish inversions with or without mode ${}_3S_2$. We therefore consider a total of six subsets of modes, each of which yields separate inversion results, which we compare. Tables 2 and 3 summarize our nomenclature: models are designated by a number (1-6, Table 3), indicating the subset of data used, and an index (a-z, i1,i2,i3, Table 2), indicating the type of model parametrization in the core.

3. Fits to c_2^0 Data

The fits to the different subsets of data, corrected for crustal effects, for some representative model parametrizations, are presented in Figure 3a (mantle and outer

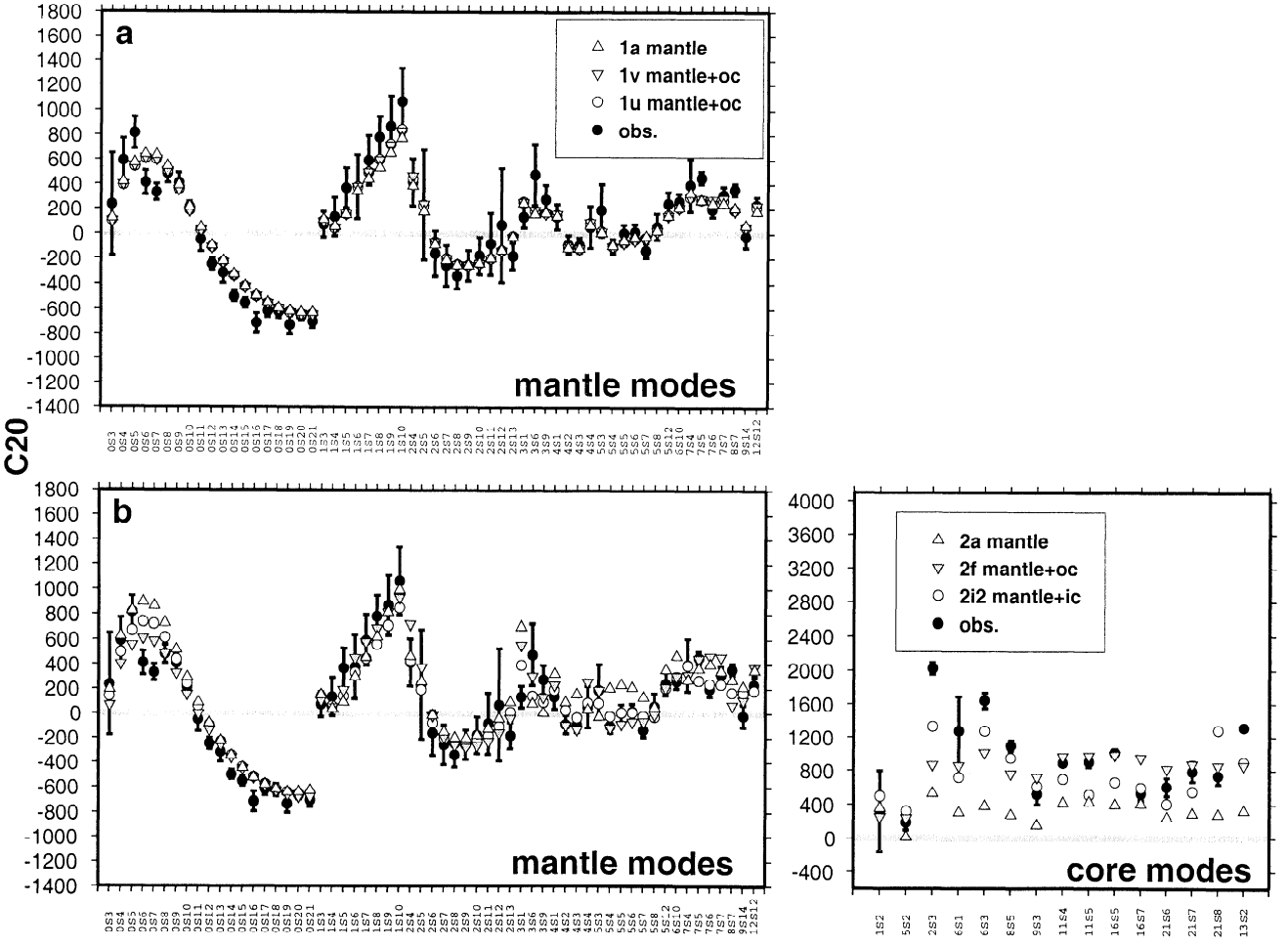

Figure 3. Comparison of observed and predicted c_2^0 splitting coefficients for models obtained using different subsets of modes: (a) modes with sensitivity to the mantle and outer core only (models "1"). Different models are indexed as indicated in Table 2; $1a$, mantle only; $1u$, four layers in the outer core; and $1v$, six layers in the outer core. (b) Mantle, outer core, and ic1 modes. (c) and (d) mantle, outer core, and ic2 modes, without ${}_3S_2$ (Figure 3c) or with ${}_3S_2$ (Figure 3d). The predictions of three models are shown in Figures 3b, 3c and 3d: $2a, 3a, 4a$, mantle structure only; $2f, 3f, 4f$, mantle with one layer spanning the outer core; $2i2, 3i2, 4i2$, mantle plus depth dependent transverse isotropy in the inner core. When the prediction of the anisotropic model is not visible, it means it is identical to that of the mantle only model. Error bars indicate measurement errors. When they are not visible, they are smaller than the size of the symbol.

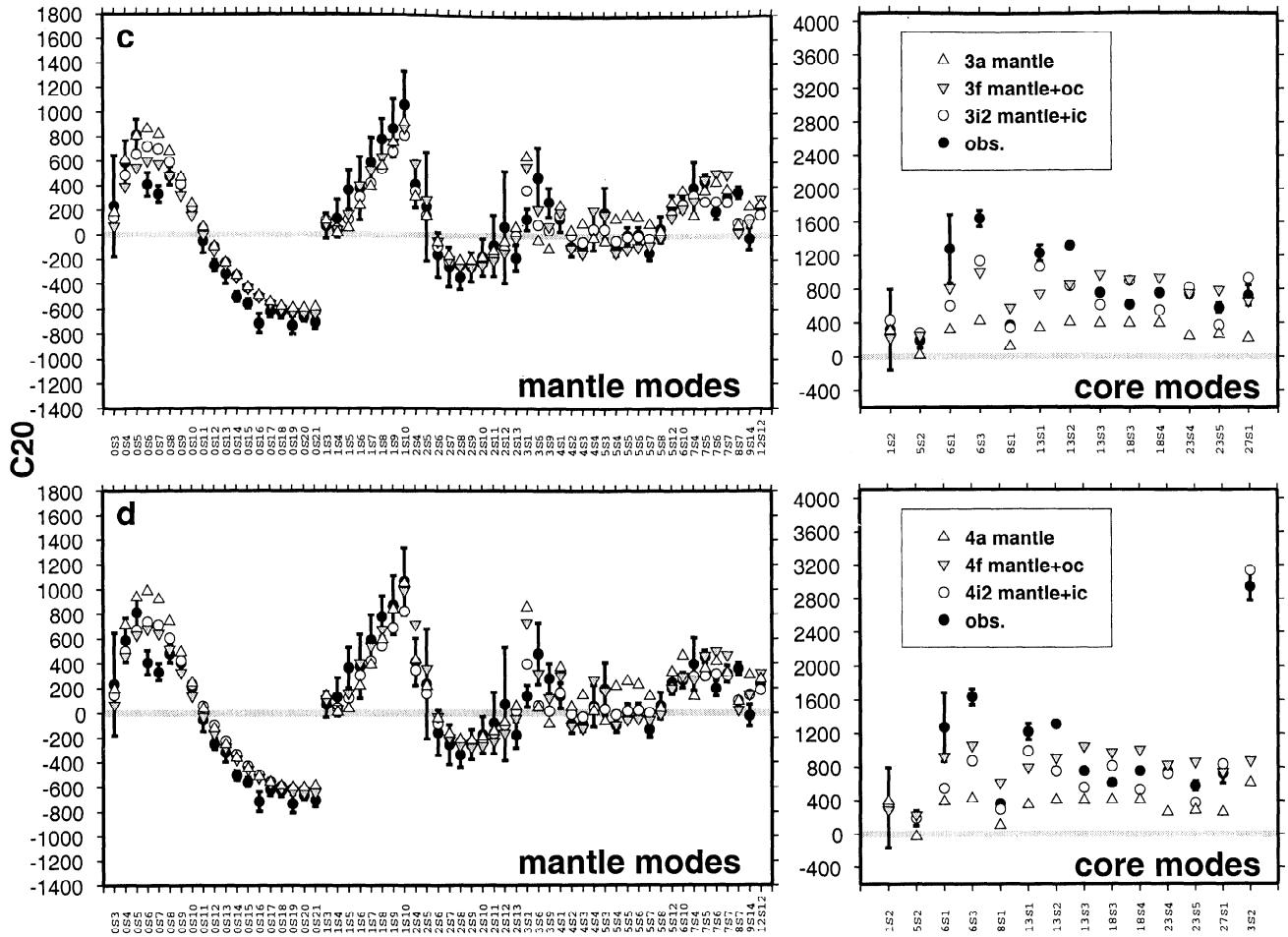

Figure 3. (continued)

core (oc) modes only), Figure 3b (mantle, oc, and ic1 modes), Figure 3c (mantle, oc, and ic2 modes, without ${}_3S_2$), Figure 3d (mantle, oc, and ic2 modes, with ${}_3S_2$) and Figure 4 (all modes; Figure 4a, without ${}_3S_2$ and Figure 4b with ${}_3S_2$). In Figure 3a we present comparisons of fits for three models: a model restricted to the mantle ($1a$), and two models with four ($1u$) and six ($1v$) layers respectively in the outer core. We note that adding structure in the outer core minimally improves the fit compared to the mantle only model $1a$. In Figures 3b, 3c, 3d 4a and 4b, comparisons of fits are shown for three models: (1) a model restricted to the mantle (models $2a, 3a, 4a, 5a, 6a$respectively), (2) a model with the same mantle parametrization plus one layer spanning the outer core (models $2f, 3f, 4f, 5f, 6f,$) and (3) a model with the mantle as above plus depth-dependent transverse isotropy in the inner core (models $2i2, 3i2, 4i2, 5i2, 6i2$).

The following points can be made from Figures 3 and 4. In all cases, the mantle-only model a provides a significantly poorer fit to the ${}_4S$ and ${}_5S$ mantle mode branches, than models in which core structure is allowed. For core-sensitive modes, both inner-core anisotropy and outer core structure improve the fits with respect to a mantle-only model, but underpredict the splitting of ${}_2S_3$, ${}_6S_1$, ${}_6S_3$, ${}_8S_5$ and ${}_{13}S_2$. Whether or not ${}_3S_2$ is included (Figures 3c,d and 4a,b) does not change the general pattern of fit to the other core modes. The outer core models most significantly underpredict the splitting of ${}_3S_2$.

The fits to our toroidal mode data set are shown in Figure 4c. They are not great whichever model is considered, and including the toroidal modes systematically increases the residual variances in the inversion. This could be largely due to the uncertainties in the toroidal measurements.

Overall, the fit of the outer core models is at least as good as that of models with inner core anisotropy, except for mode ${}_3S_2$. This is summarized in Figure 5, which compares residual variance plots for the five families of modes with inner core sensitivity shown in Figures 3 and 4, as a function of model parametrization, following Tables 2 and 3. We here compare models with only mantle structure (a), with mantle and outer core structure ($b - z$) and with mantle structure plus inner core anisotropy ($i1, i2, i3$). When mode ${}_3S_2$ is excluded, (Figure 5a, 5b and 5c), the residual variance is comparable for models with outer core structure extending throughout the outer core, even though the number of parameters in the inversion is smaller than when inner

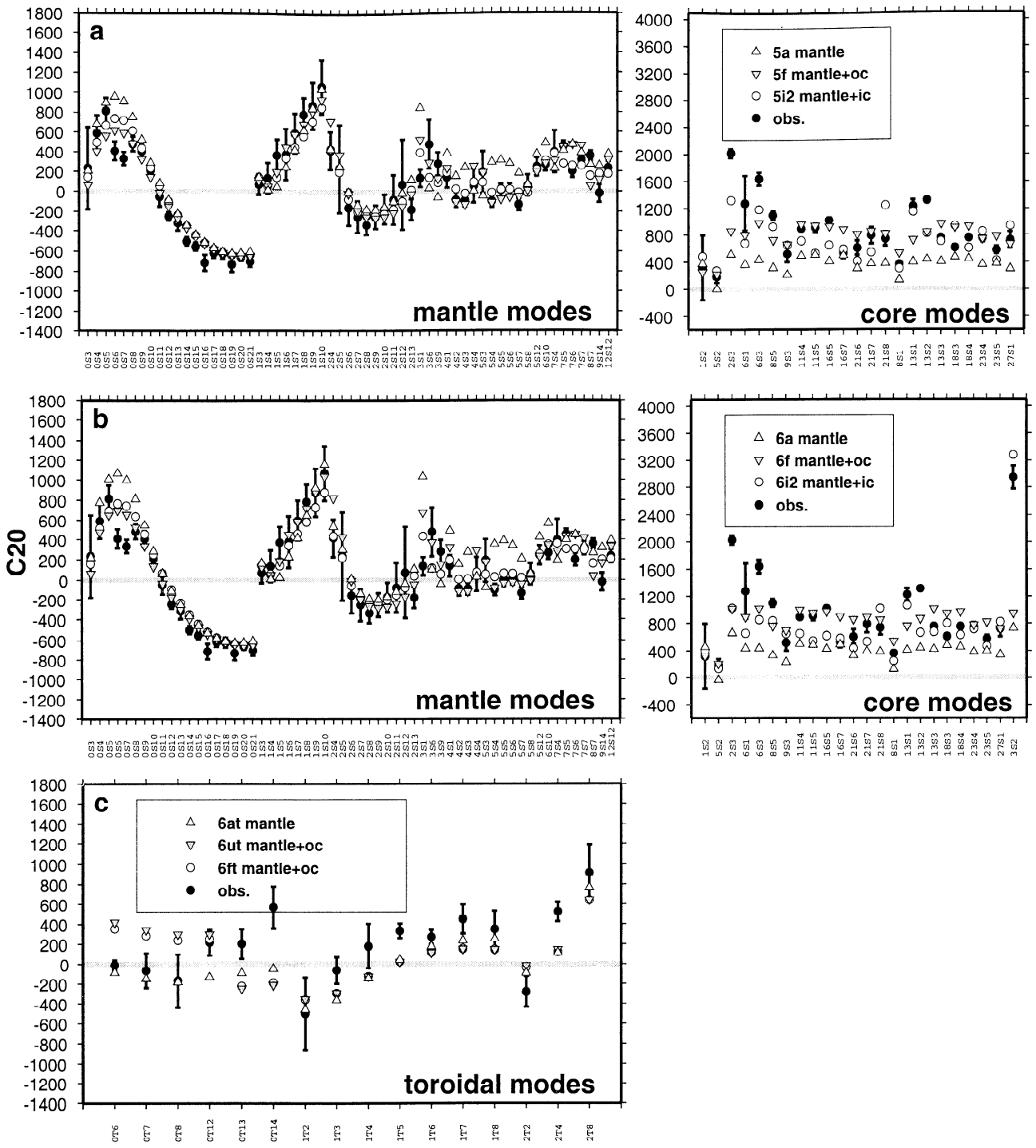

Figure 4. Figures 4a and 4b are same as Figure 3c and 3d when all modes are considered: (a) without ${}_3S_2$, models (5a,5f,5i2); (b) with ${}_3S_2$ (models 6a,6f,6i2) and (c) toroidal modes, models 6at, 6ut, 6ft

core anisotropy is considered. Only by including ${}_3S_2$ do we obtain a significantly better fit for models with inner core anisotropy. It is clear that the exceptionally large splitting of mode ${}_3S_2$ dominates the variance results, a well-known bias of standard least squares inversions. We have also considered models with inner core heterogeneity rather than anisotropy, which provide fits comparable to those obtained with a layer at the bottom of the outer core (such as models z).

4. The c_2^0 Depth Profiles

Depth profiles obtained in the mantle and outer core for the models corresponding to Figures 3 and 4 are shown in Figures 6 and 7. In all cases except Figures 6a and 6b, a comparison is shown between models restricted to the mantle ($1a - 6a$), models with depth dependent inner core anisotropy ($1i2 - 6i2$) and models with four layers in the outer core ($1u - 6u$). In Figures

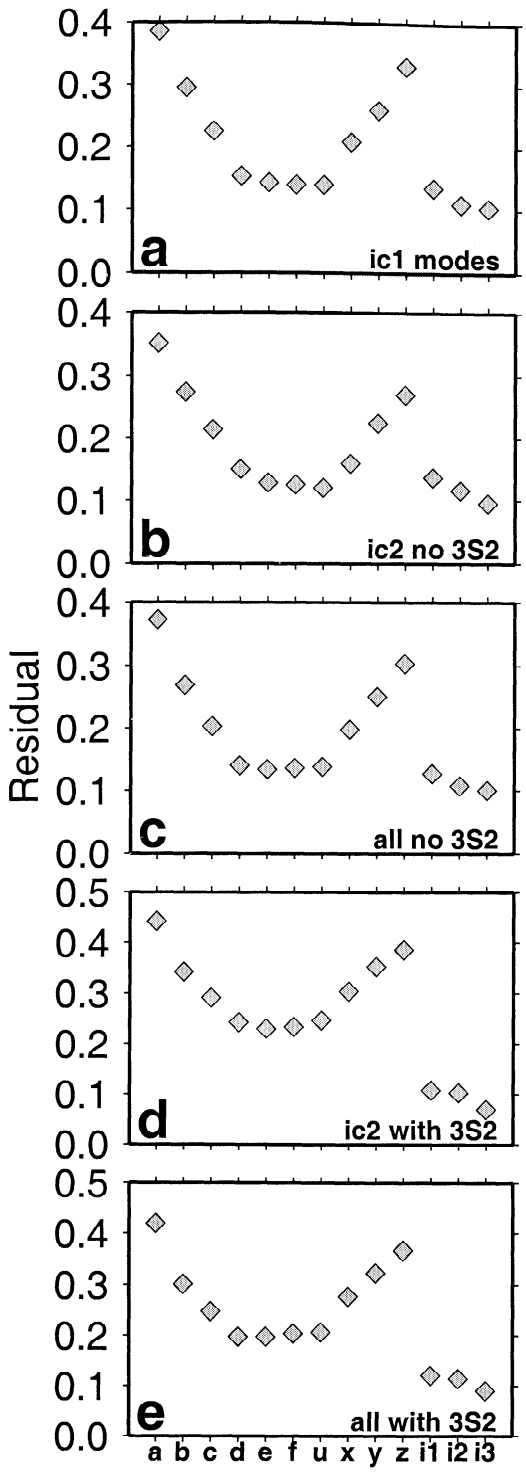

Figure 5. Residual variances for c_2^0 as a function of model parametrization for the different subsets of data considered: (a) mantle, outer core, and ic1 modes; (b) mantle, outer core, and ic2 modes, without ${}_3S_2$; (c) all modes without ${}_3S_2$; (d) same as Figure 5b, with ${}_3S_2$; and (e) all modes with ${}_3S_2$.

6a and 6b, the inner core anisotropy model is replaced by a model with six layers in the outer core ($1v - 2v$).

Comparison of the V_s profiles for models restricted to the mantle ($1a - 6a$) and models which allow for structure in the outer core show that the c_2^0 profile in V_s is stable throughout the mantle, regardless of the subset of modes used. Note that at the bottom of D" (depth range 2650-2891 km), models with outer core structure consistently show a larger positive V_s perturbation, compared to models with inner core anisotropy, in better agreement with c_2^0 profiles obtained using tomographic waveform inversions (e.g., SAW12D, Figure 6b ot 6d).

V_p profiles are also generally stable in the mantle, with respect to the mode subset used. When inner core sensitive modes are included, models restricted to the mantle have excessive fluctuations with depth compared to the case when only mantle modes are inverted. Models with inner core anisotropy have V_p profiles most compatible with those obtained when no inner core sensitive modes are used (Figure 6a). On the other hand, density profiles are more stable with respect to the mode subset when outer core structure is allowed. Inner core anisotropy models (Figure 6c, 6d, 7a, 7b) produce negative c_2^0 in ρ in the last 700 km of the mantle, a feature not seen in models obtained only with mantle modes (Figure 6a).

Comparing the V_s, V_p, and ρ profiles in the mantle when all modes are considered (Figures 7a and 7b), we find that ρ tends to follow V_s throughout the mantle, whereas V_p is not correlated with V_s or ρ below a depth of about 1900 km. This is also found for other large degree 2 coefficients (c_2^2, s_2^2) and will be reported in more detail elsewhere.

The outer core models shown in Figures 6, 7a and 7b are also generally consistent from one family of modes to the next. They consistently indicate a positive V_p perturbation associated with a negative ρ perturbation, both decreasing with depth from the CMB, indicating a possible concentration of heterogeneity near the top of the outer core. Adding mode ${}_3S_2$ (Figures 6d and 7b) yields V_p profiles in the outer core that are more regularly decreasing with depth. The outer core model obtained using mantle and outer core modes alone shows the same trends.

Figures 7c and 7d illustrate the stability of our results with respect to two important aspects of parametrization in the mantle and outer core. The first one is CMB topography. In Figures 6, 7a and 7b, CMB topography is allowed, and the resulting c_2^0 is of the order of 3 ± 1 km, which is large compared to astronomical predictions [*Gwinn et al.*, 1986]. Figure 7c shows c_2^0 depth profiles in V_s, V_p, and ρ when CMB topography is not allowed, for the complete data set (including ${}_3S_2$). There is practically no difference, except for the model which is confined to the mantle, and shows a larger perturbation in D". The variance reductions are somewhat lower when CMB topography is not allowed.

In the model shown Figure 7d, on the other hand, we have constrained the outer core structure in such a way that no lateral variations in density are allowed (but CMB topography is allowed). Here we compare a mantle model ($6a2$) with two outer core models ($6f2$

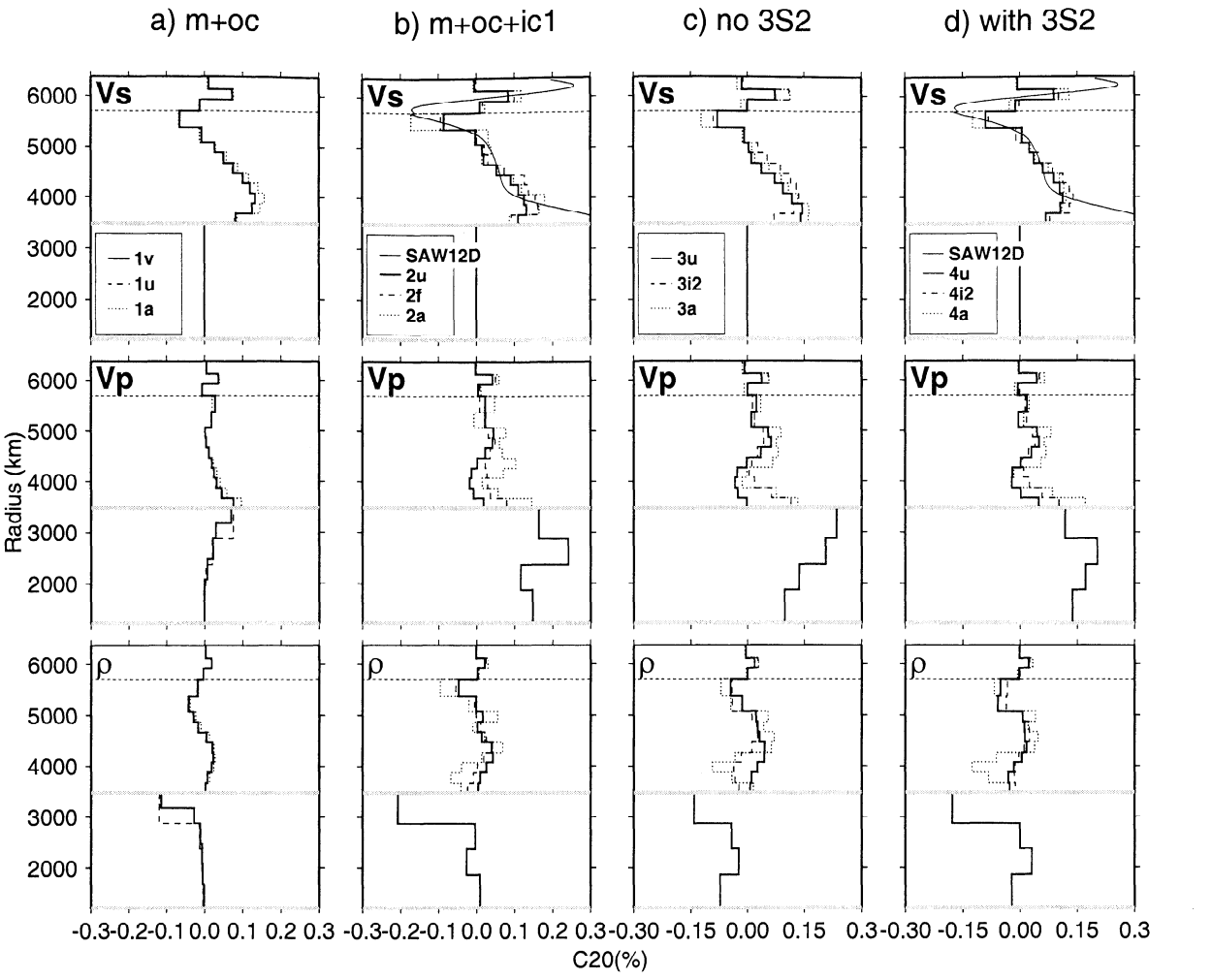

Figure 6. The c_2^0 depth profiles through the mantle and outer core, in (top)V_s (middle) V_p and (bottom) ρ corresponding to inversions performed using different subsets of modes: (a) mantle and outer core sensitive modes only; (b) mantle, outer core, and "ic1" modes; (c) mantle, outer core, and "ic2" modes, without ${}_3S_2$; (d) same as Figure 6c including ${}_3S_2$ in the inversion. Labeling of models follows Tables 2 and 3. Models labeled a allow for structure only in the mantle. Models labelled $i2$ include depth dependent anisotropy in the inner core. Models labelled u include four layers in the outer core. In Figure 6a, model v includes six thinner layers in the outer core. Variations with depth of the three parameters are given in percent deviations from zero, referred to the reference PREM model. V_p and ρ are kept proportional to V_s in the upper mantle.

and $6u2$). This has no incidence on the mantle profiles, compared to Figure 7b, but increases the strength of c_2^0 in V_p in the top two layers of the outer core, for the four layer outer core model $6u2$. The residual variance is consistently larger in this case than when density is allowed to vary in the outer core.

In Figures 8a-8d we show the depth profiles obtained when toroidal modes ${}_1T_2$-${}_1T_8$, ${}_2T_4$, ${}_2T_6$,${}_2T_8$, and ${}_0T_6$-${}_0T_8$, ${}_0T_{12}$-${}_0T_{14}$ are added to our collection of spheroidal modes, including only mantle and outer core modes (Figure 8a), mantle, outer core, and ic1 modes (Figure 8b); and finally all spheroidal modes (Figures 8c and 8d), respectively. We note no significant changes in the resulting profiles, compared to Figures 6 and 7, except in the case when only mantle modes are inverted: the V_p and ρ profiles resemble more closely those obtained with core modes, indicating that in this case, adding toroidal modes improves the resolution of structure in the lower mantle. We also note that the V_s profile just below the 670-km discontinuity is in better agreement with SAW12D (in amplitude) and that the V_p profile, in the same depth range, shows better correlation with V_s, so that toroidal modes do improve resolution in the mid mantle as well. The trends in variance reductions and fits to the mode splitting data set are the same with or without toroidal modes, but the general level of variance reduction is poorer when the toroidal modes are added, an indication that the toroidal data are noisy.

Finally, in Figure 9 we examine the influence on core structure of two important assumptions: (1) crustal cor-

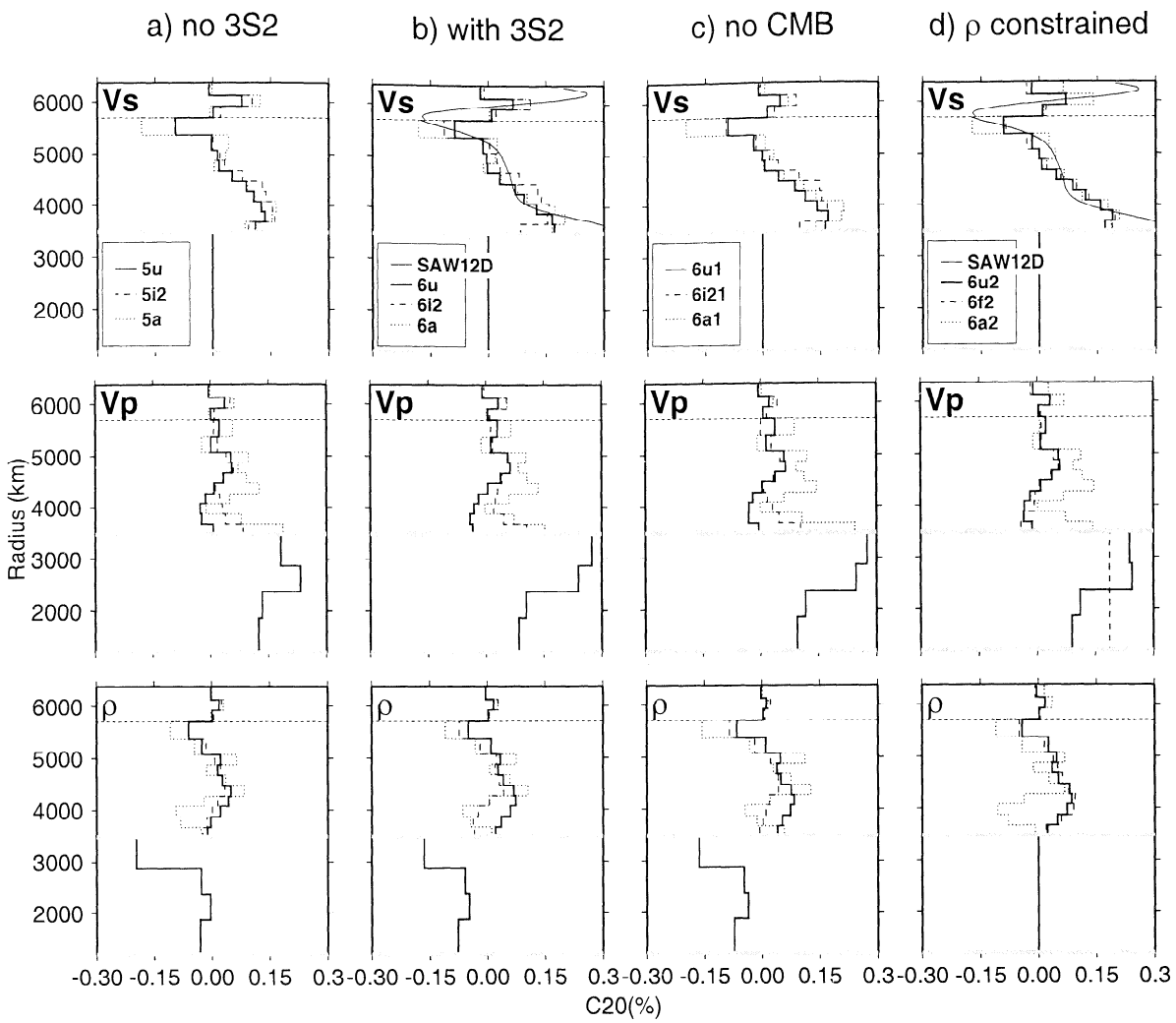

Figure 7. (a)(b) Figures 7a and 7b are same as Figure 6 for inversions that include all modes, (a) without ${}_3S_2$ or (b) with ${}_3S_2$. (c) All modes included, CMB topography not allowed. (d) CMB topography allowed but density constrained to be hydrostatic in the outer core. The V_s profile in c_2^0 for the *SH* model SAW12D [*Li and Romanowicz*, 1996] is given for comparison in Figures 7b and 7d.

rections and (2) constraints on the ρ profiles in the mantle. The entire mode data set is used in these inversions, and we allow for CMB topography. The crustal model used to correct data in the inversions shown in Figures 6-8 is a simple ocean-continent model of topography, bathymetry, and Moho depth which we previously used as starting model in our construction of model SAW12D [*Li and Romanowicz,* 1996]. Figures 9a and 9b show depth profiles in c_2^0 obtained when no crustal corrections are applied, while Figures 9c and 9d have crustal corrections applied. Figure 9a corresponds to the same parametrization as in Figure 7b, and the comparison indicates that crustal corrections have little effect on the structure obtained in the lower mantle and the core. In the case shown in Figures 9b and 9c we constrain the density profile in the lower mantle to be proportional to V_s, with the same ratio as in the upper mantle. Comparison of Figure 9b and 9c illustrates how crustal corrections do not have any incidence on the features of our models in the deep mantle and core. Whether or not lateral heterogeneity in density can be resolved in the mantle from normal mode data is the subject of controversy [e.g., *Resovsky and Ritzwoller*, 1999; *Ishii and Tromp*, 1999]. Comparison of Figures 9a and 9b shows that the V_s and V_p profiles are stable, whether or not ρ is inverted for independently. Finally, Figure 9d shows the results of an inversion in which both V_p and ρ are constrained to be proportional to V_s throughout the mantle. While other features of the depth profiles are stable, the comparison of Figures 9c and 9d emphasizes the lack of correlation in the depth fluctuations of V_p and V_s in the lower half of the lower mantle, when V_p is solved for independently. Generally, Figure 9 shows that parametrization in the mantle and crustal corrections have little incidence on the profiles in V_p and ρ obtained in the outer core. Likewise, fits to the data

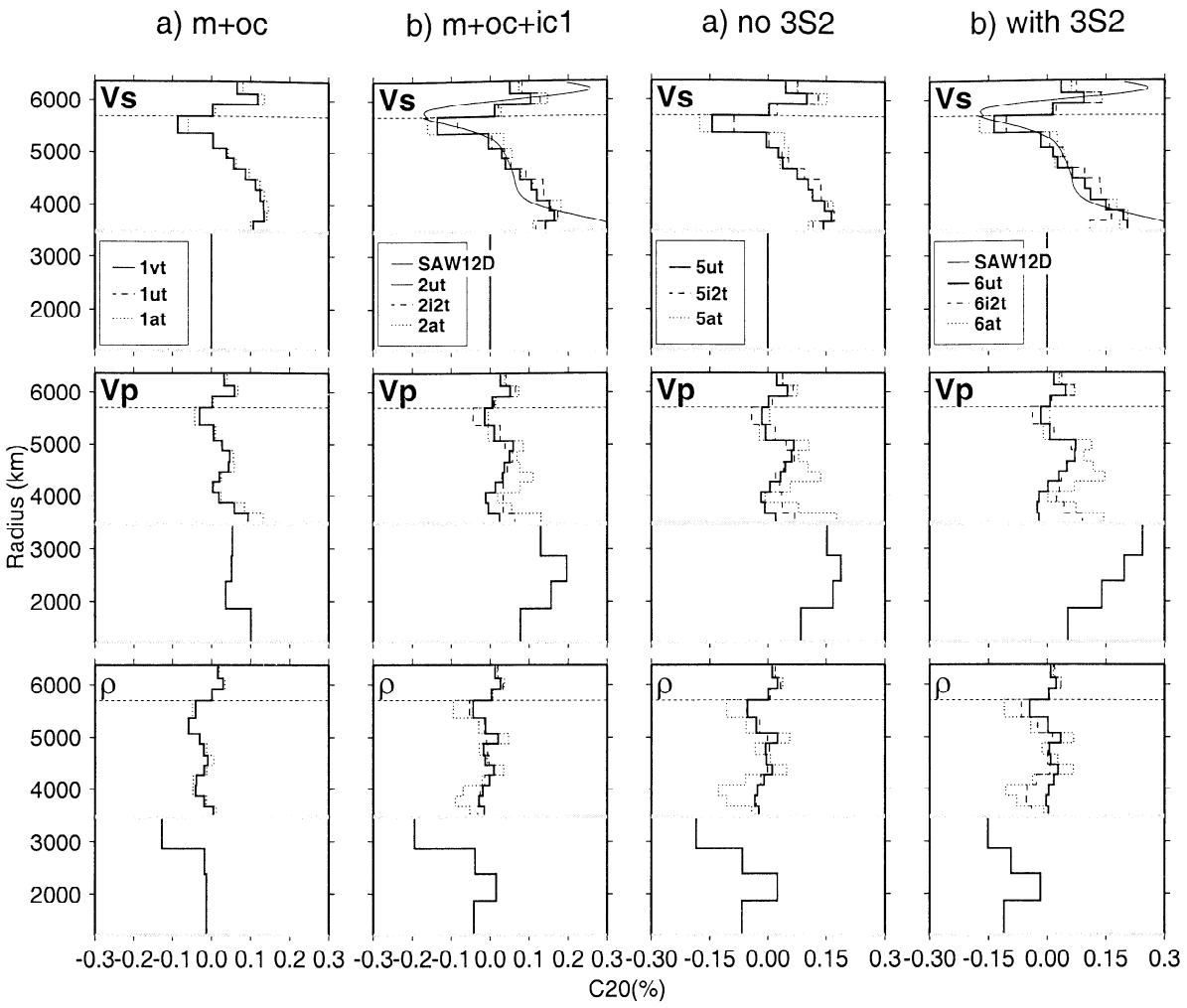

Figure 8. Same as Figures 6 and 7 for the case when toroidal modes are included in the inversion. (a), (b), (c), (d) Same spheroidal mode data sets as Figures 6a, 6b, 7a and 7b, respectively.

and variance reductions, although poorer for the cases shown in Figure 9, do exhibit the same trends as shown in Figure 5.

Figure 10 shows the transverse isotropy models in the inner core ($2i1, 2i2$), without and with depth dependence respectively, obtained when different families of spheroidal modes are considered. P wave anisotropy (ϵ) has an amplitude of 1% on average. When depth dependence is allowed, anisotropy is very weak at the top of the inner core, in agreement with some recent body wave studies, and it peaks at a depth of about 200km in all cases except $2i2$ (ic1 modes). There is more variability in the other anisotropic parameters (σ and γ), but those are very poorly constrained. Likewise, anisotropy in the central part of the inner core is poorly constrained with mode data alone, so that the variability in ϵ below a depth of 600 km in the inner core does not have any significance. Overall, the anisotropic models obtained, like the outer core models, are consistent with each other, regardless of the subset of modes considered.

The same inversion procedures as described above for c_2^0 have been applied to the four remaining degree 2 coefficients, using data from *He and Tromp* [1995] and *Resovsky and Ritzwoller* [1998]. While the results will be discussed in detail elsewhere (B. Romanowicz, manuscript in preparation, 2000), it is important to assess whether the reconstructed degree 2 mantle models obtained using the complete mode data set present any unacceptable features when inner core anisotropy is not included. Plate 1 shows maps of degree 2 perturbations in V_s, V_p and ρ at selected depths in the lower mantle, for a parametrization with one outer core layer spanning the outer core, allowing V_p to vary independently of V_s in the lower mantle, but with ρ proportional to V_s throughout the mantle. As found in other tomographic studies, the l=2, m=2 structure dominates the V_s and V_p maps down to 1500 km, with fast velocities associated with circum-Pacific regions of slab subduction. At the bottom of the mantle the influence of c_2^0 is more marked, especially in V_s, producing the characteristic "ring of high velocities" around the Pacific.

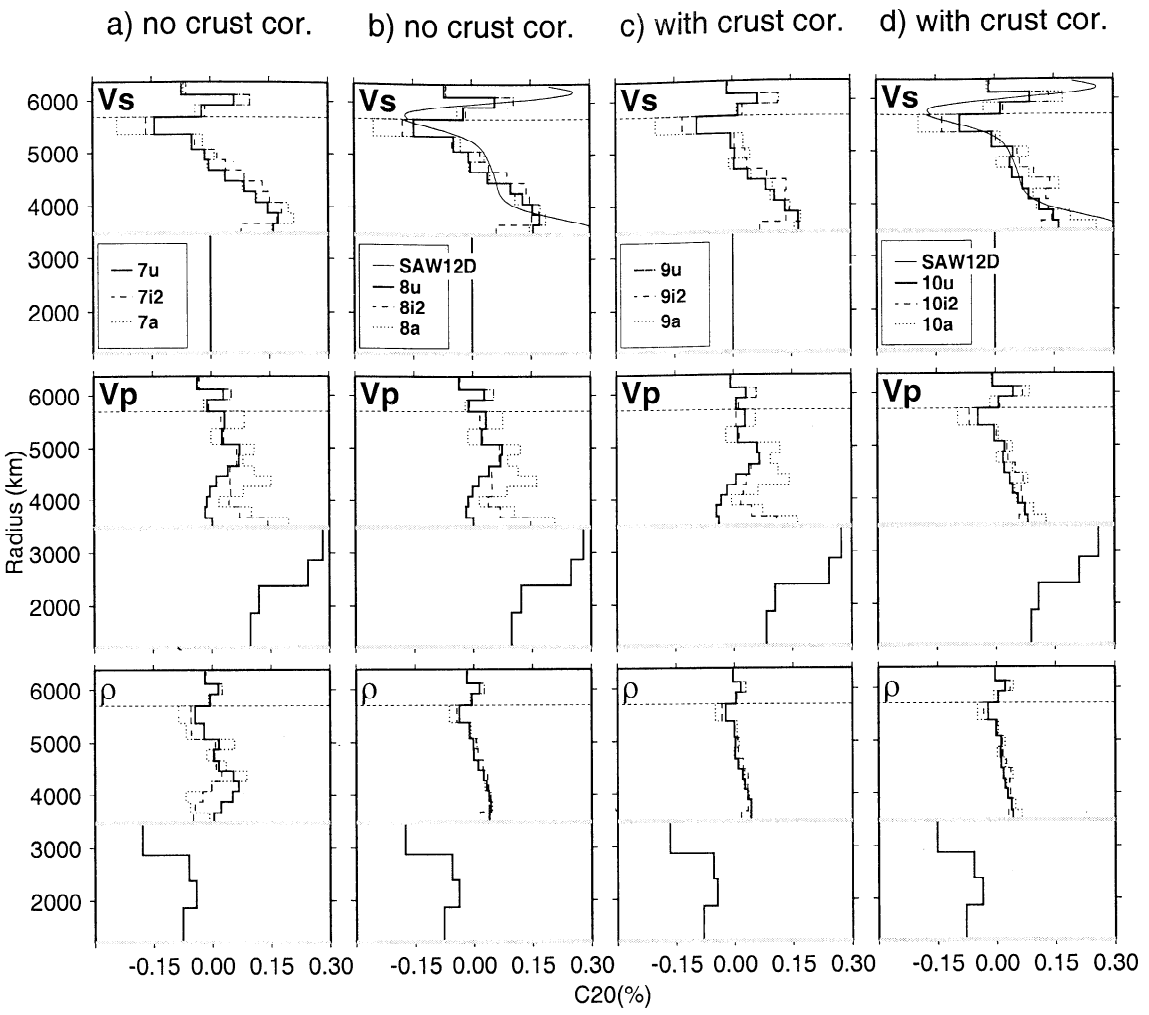

Figure 9. Same as Figure 7b (all modes inverted simultaneously) when the constraint of proportionality of V_p and ρ to V_s is relaxed below a depth of 450 km. We compare results without (a)(c) and with (b)(d) crustal corrections, and with (a)(b) and without (c)(d) CMB topography. Relaxing the constraint of proportionality changes the V_p profile in the 450-1000 km depth range, and makes the ρ profile less smooth, but has no incidence on the lowermost mantle and outer core profiles.

5. D" Versus Outer Core Structure

An important question is whether it might be possible to explain the anomalous core mode splitting by structure confined to the deep mantle, especially since recent studies have shown evidence for strong heterogeneity in D" [*e.g. Garnero and Helmberger,* 1995, 1996; *Bréger and Romanowicz,* 1998; *Ritsema et al.,* 1998]. Previous authors have pointed out that this is not possible, since the c_2^0 of mantle modes that do not exhibit large splitting would then be overestimated. We have confirmed this by conducting a systematic forward modeling experiment, searching for models with independent structure in V_s, V_p and ρ in D". We illustrate the results in Figure 11, where we show the predictions of several representative models with structure confined to D" only. Figure 11 illustrates the fact that strong heterogeneity is needed in D" to reach the level of splitting observed for ic1 and ic2 modes. On the other hand, when this heterogeneity is strong, the splitting of modes sensitive to V_p in the mantle (branches ${}_0S$, ${}_1S$, and ${}_5S$ in particular), is overestimated.

Finally, Figure 12 shows the fit to c_2^0 splitting coefficients of three different one layer models of outer core structure (all spanning the depth range 2891-4500 km) which give a good fit to the average level of splitting of outer core modes. From Figures 11 and 12 we see how outer core structure trades off with D" to explain the splitting of ${}_1S$ modes (and low-order ${}_0S$ modes) but does not contribute to the splitting of ${}_5S$. The difference between the three outer core models considered is only in the $d\ln V_p/d\ln\rho$ ratio, to which the ${}_1S$ branch is sensitive, but also, significantly, mode ${}_3S_1$. We see that the absence of splitting of this particular mode is not incompatible with outer core structure when an appropriate ratio $d\ln V_p/d\ln\rho$ is chosen. Whereas our inversion results, which are designed to simultaneously fit many modes, do not predict the correct splitting of

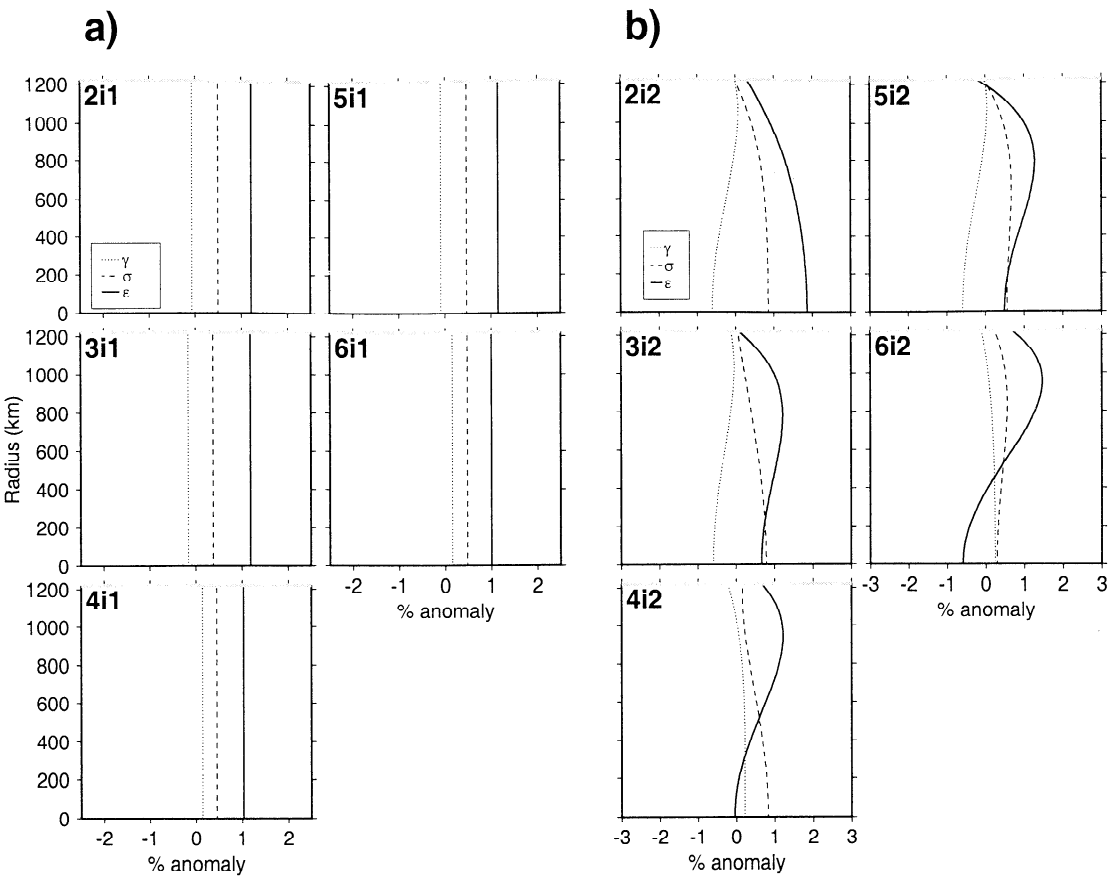

Figure 10. Profiles, as a function of depth in the inner core, for transversely isotropic models obtained with the different data sets of the following anisotropic parameters: ϵ=$\frac{1}{2}$(C-A)/A; σ=$\frac{1}{2}$(L-N)/A; γ=-$\frac{1}{4}$($\frac{1}{2}$ A+$\frac{1}{2}$C-2L-F)/A, where A,C,F,L,N have the standard definitions. (a) Constant transverse isotropy models. (b) Depth-dependent transverse isotropy. Model numbering is as in Figures 3 and 4. 2i1 and 2i2, models obtained using mantle plus outer core plus ic1 modes; 3i1 and 3i2, mantle plus outer core plus ic2 modes without ${}_3S_2$; 4i1 and 4i2, mantle plus outer core plus ic2 modes with ${}_3S_2$; 5i1 and 5i2 : all modes without ${}_3S_2$; 6i1 and 6i2, all modes with ${}_3S_2$.

${}_3S_1$(e.g. Figures 3 and 4), Figure 12 indicates that more refined forward modeling can do it.

6. Discussion

From the experiments described above we draw the following conclusions. While models including inner core anisotropy provide an improvement over "mantle-only" models to explain anomalous splitting of core sensitive modes, simple models involving outer core structure perform at least as well when mode ${}_3S_2$ is excluded from the data set. On the other hand, mantle structure and, in particular, large c_2^0 in D" alone cannot consistently account for the observed splitting of all modes, requiring excessive splitting in the P mode branches ${}_4S$ and ${}_5S$.

From the above results, it follows that the interpretation of anomalous splitting of core modes in terms of inner core anisotropy relies heavily on one single mode, ${}_3S_2$, which has the largest splitting and the largest sensitivity to inner core anisotropy (mode ${}_7S_2$ may present similar features (G. Masters, personal communication, 2000). We argue that, in the presence of over 20 modes sensitive to inner core structure, a model that improves the fit to one mode only, an effect clearly related to the use of an L2 norm in the inversion, should be viewed with caution. When this mode is removed, models with outer core structure provide similar levels of fit to the data, and V_s and ρ profiles that are in better agreement with those obtained using data sensitive only to mantle structure. On the other hand, the V_p structure obtained with inner core anisotropy indicates a stronger C20 component in D", which seems to be more compatible with other V_p studies [e.g., *Obayashii and Fukao*, 1997]. Discrimination between outer core heterogeneity and inner core anisotropy based on mantle c_2^0 structure is therefore inconclusive.

The issue of outer core heterogeneity has generated strong debate. Numerous seismological studies based on body wave data have attempted to resolve it [e.g., *Lay*

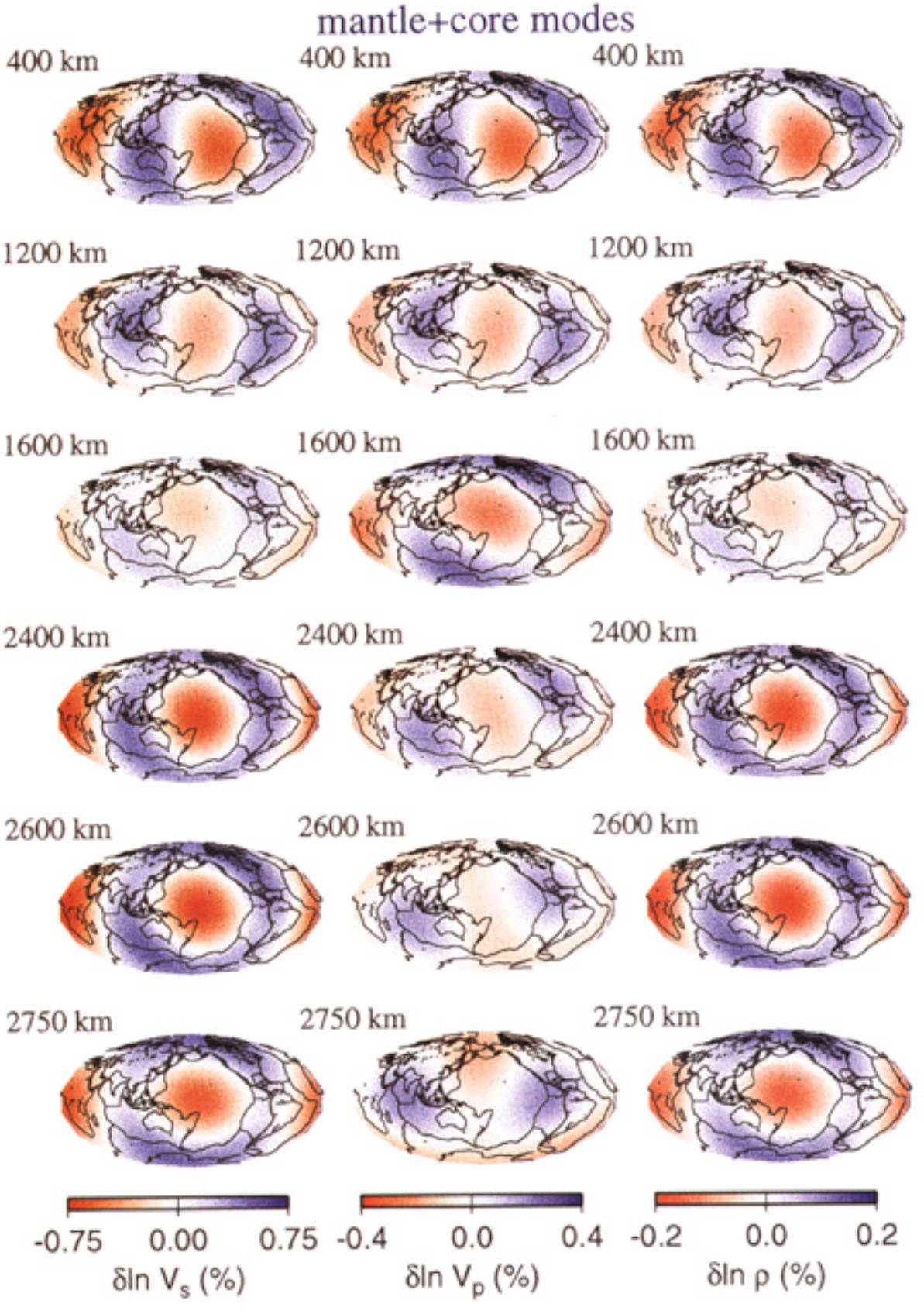

Plate 1. Maps of reconstructed degree 2 heterogeneity in (left) V_s, (middle) V_p and (right) ρ at representative depths in the mantle mantle, obtained by combining the results of inverting all five degree 2 coefficients. The model shown has been constructed using the complete spheroidal data set and allowing for one layer spanning the entire thickness of the outer core (model $7f$ shown in Figure 9a).

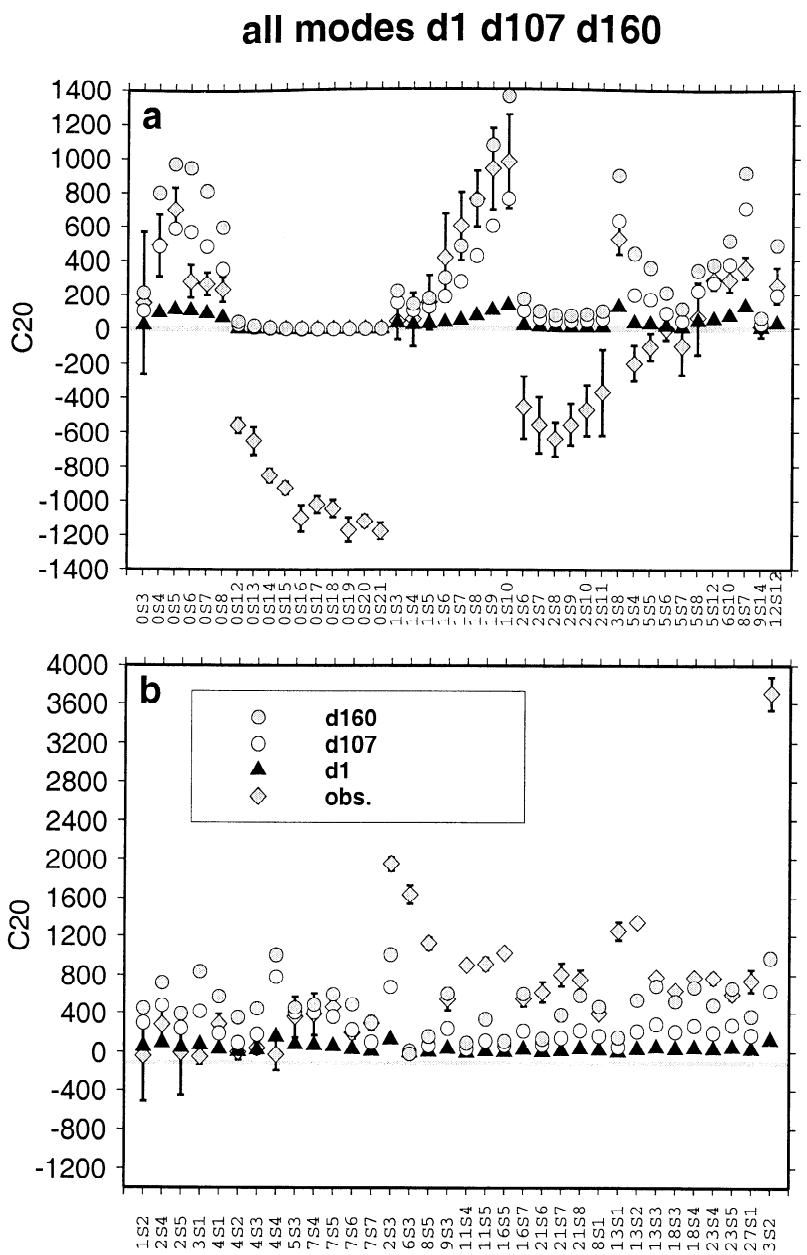

Figure 11. Comparison of c_2^0 data and predictions for (a) mantle modes and (b) core modes, for several representative models consisting of a single, 300 km thick, layer of heterogeneity in D", in which V_s, V_p, and ρ are allowed to vary independently. The c_2^0 amplitudes in V_s, V_p and ρ are 1%, 0.5%, and 0.25% respectively, for model "d1", 5%, 3%, and 1% respectively for model "d107", and 6%, 6%, and 4% respectively, for model "d160".

and Young, 1990; *Souriau and Poupinet,* 1990; *Tanaka and Hamaguchi,* 1993; *Kohler,* 1995; *Vasco and Johnson,* 1998]. The models we present here appear to require significant structure in density in the outer core. However, the depth dependence of this density variation is not well resolved. The simplest, one layer models, require on the order of 0.03% of negative c_2^0 in density throughout the outer core, with corresponding positive c_2^0 in V_p, of similar magnitude. While difficult to argue for from a standard geodynamics point of view [*Stevenson,* 1987], we note that this particular relation between V_p and ρ is what would be expected if the light elements in the outer core [*e.g. Poirier,* 1994], were confined to a particular region with strong zonal geometry. Such a region could potentially be the interior of the tangent Taylor cylinder of hydrogeomagnetic core models [*Glatzmeier and Roberts,* 1995; *Hollerbach and Jones,* 1995]. Indeed, present models of core dynamics clearly distinguish between the structure inside and outside the tangent cylinder, as the character of the fluid motion appears to be much different in these two regions. However, particularly strong forces would have

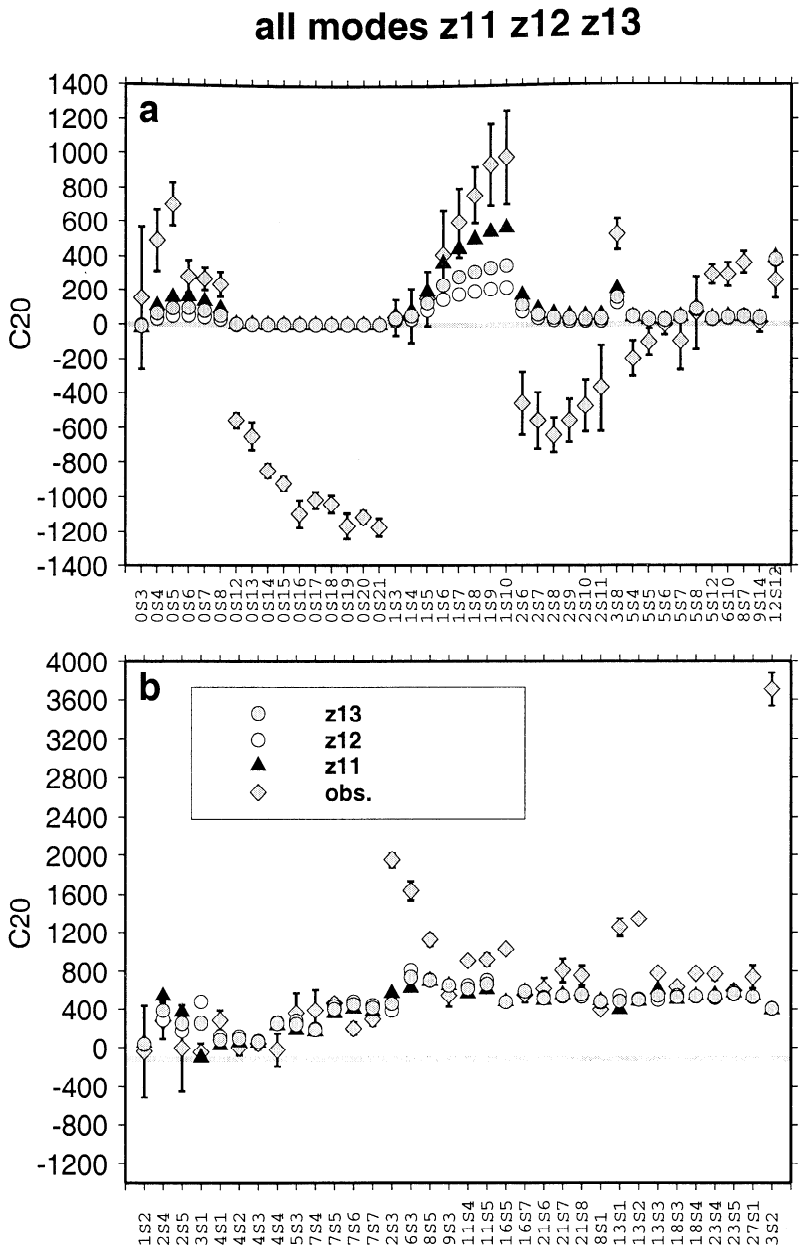

Figure 12. Comparison of c_2^0 data and predictions for (a) mantle modes and (b) core modes, for several representative models consisting of a single, 1500 km thick layer of heterogeneity at the top of the outer core, in which V_p and ρ are allowed to vary independently. The c_2^0 profiles have been constructed from the spherical harmonics expansion of a model in which heterogeneity is confined inside the Taylor cylinder tangent to the inner core (see Figure 13), where perturbations in V_p and ρ are 1%, and -1.8% respectively, for model "z11", 1% and -0.5% respectively for model "z12" and 1% and -1% respectively for model "z13". Note the sensitivity of modes ${}_1S_7$-${}_1S_{10}$ and mode ${}_3S_1$ to the ratio between V_p and ρ.

to be invoked in order to keep the light material from flowing out of the tangent cylinder. Present dynamic models of the outer core do not address this issue.

On the other hand, when more flexibility is allowed in the inversion by introducing several layers, the density structure that is recovered is largest at the top of the core, decreasing to negligible amounts in the middle of the outer core. There appear to be some more variability regarding the depth profile of the corresponding V_p structure, but in all cases, it is of opposite sign and also decreases with depth. We have examined models where density c_2^0 is constrained to be zero (or hydrostatic) in the outer core, but such models provide significantly poorer fit to the data. An outer core layer near the CMB with density anomaly of a fraction of a percent, with corresponding positive V_p anomaly is

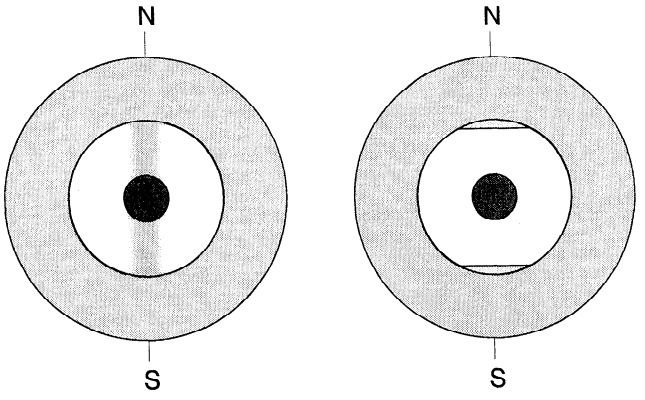

Figure 13. Conceptual sketches showing the two alternative outer core models discussed in the text: a) heterogeneity confined to the Taylor cylinder tangent to the inner core; (b) stagnant polar "caps" in the outer core.

arguably a more realistic model of the outer core and it would be compatible with models of stagnant layers at the top of the outer core [*Braginsky,* 1963, 1993; *Lister and Buffett,* 1998]. The data do not allow to constrain the thickness of this layer with any accuracy, even though inversions tend to favor thicknesses in excess of 500 km. This may be due to the poor depth resolution of core modes in the outer part of the core. We note that this type of model is also compatible with the results obtained by *Souriau and Poupinet* [1990] using differential $SKS - SKKS$ travel times, although they have later proposed that contamination from D" may weaken their interpretation [*Souriau and Poupinet,* 1991].

The variance reduction plots in Figure 5 compare the results for one-layer models of the outer core with increasing thickness, starting from the top $(b - u)$ or the bottom of the outer core $(x - z$, see also Table 2). These plots indicate a preference for heterogeneity that extends over a large thickness in the outer core (models d to u). In particular, the heterogeneity does not seem to be confined in a thin layer either at the top or the bottom of the outer core. This would favor the interpretation in terms of heterogeneity associated with the tangent Taylor cylinder (Figure 13), rather than a stagnant layer, the thickness of which is unlikely to be larger than a few hundred kilometers [*Wahr and De Vries,* 1989; *Braginsky,* 1993; *Lister and Buffett,* 1998]. While such a model presently has no other physical justification, we have verified that it does not violate PKP travel time observations. An outer core model with 1% V_p increase within the tangent cylinder with respect to the reference model (a level of heterogeneity corresponding to the c_2^0 levels reported in Figures 6-9) and no heterogeneity outside the tangent cylinder produces differential $PKP(BC - DF)$ and $PKP(AB - DF)$ differential travel times well within the range of the observed residuals (Figure 14). We note that the predicted travel time residuals could also contribute to explaining the scatter in the differential travel time data. If heterogeneity is concentrated toward the top of the outer core, the predicted effects would be smaller, since the difference in path between the $PKP(DF)$ and the outer core PKP phase (AB or BC) at the bottom of the outer core is important in producing the effect shown.

If a model of outer core structure is not rejected, how then can we reconcile the large unexplained splitting of ${}_3S_2$ with such a model? We first note that there are a few other inconsistencies in the models that cannot be explained either by a simple inner core anisotropy model or by outer core structure: these concern the splitting or lack thereof of several outer core sensitive modes. Mode ${}_3S_1$ has been cited as the "problem mode" which cannot be explained together with other core modes unless inner core anisotropy is considered, since it has sensitivity to the outer core but practically none to the inner core and is not significantly split [*e.g. Li et al.,* 1991].

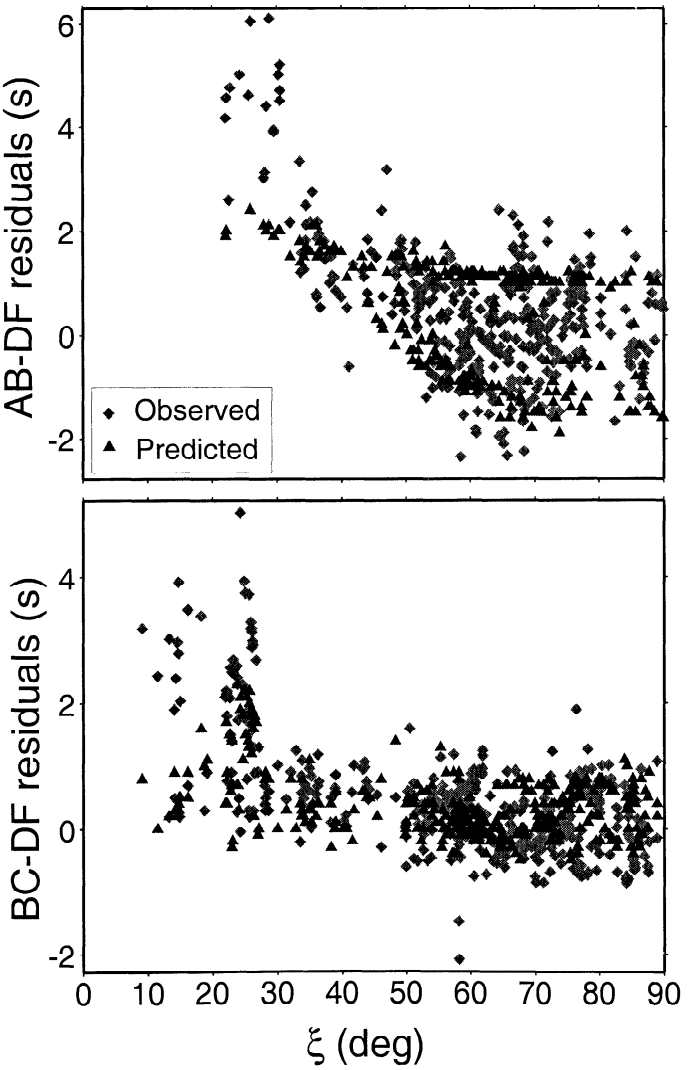

Figure 14. Comparison of observed and predicted differential travel times residuals for PKP waves, for a model of heterogeneity in the outer core consisting of 1% velocity increase inside the tangent Taylor cylinder.

From Figure 3, we see that this mode is better fit when only mantle modes are considered, than when inner core sensitive modes are added. However, inner core models fail to improve the fit to the c_2^0 of ${}_3S_1$, and we have seen that outer core models can produce a splitting of ${}_3S_1$ consistent with observations (Figure 12). The same is valid for ${}_1S_2$, which has some sensitivity to inner core structure, but small splitting.

A possibility is that some important but yet not considered effect has been neglected in the inversion. This was also suggested by Widmer et al. [1992]. In particular, we have explored the possibility of P velocity anisotropy in the outer core, as might be generated in a slurry confined to the tangent Taylor cylinder, and would not necessarily be accompanied by heterogeneity in density. The models obtained are not stable with respect to depth parametrization and generally present unrealistically large values of anisotropy (30-50%). On the other hand, on the basis of preliminary computations, ${}_3S_2$ is a mode, which together with ${}_6S_3$, another strongly split mode, also has strong sensitivity to shear velocity in the outer core. In the past, a number of authors have argued for the possibility of a small amount of shear at the top of the outer core [*Anderson and Kovach,* 1964; *Sato and Espinosa,* 1967; *Mochizuki and Ohminato,* 1989]. If a stagnant layer exists at the top of the outer core, it is not inconceivable that a small amount of shear could be present therein. In this case, core sensitivity kernels need to be recomputed for all modes and also for V_p and ρ, and we expect the sensitivity to V_p to increase and that to ρ to decrease, yielding potentially more realistic models in which, in particular, the layer at the top of the outer core could be thinner than currently estimated by our inversions. At the present time, we do not have the tools to compute lateral variations in an outer core with shear, which require a theoretical formalism that allows extremely strong heterogeneity (50-100% in shear). In the light of recent contradictions regarding simple models of inner core anisotropy, we will pursue work in this direction.

In conclusion, while inner core anisotropy cannot completely be ruled out to explain anomalous mode splitting, significantly more complex anisotropic models need to be invoked than have been so far considered, in agreement with our previous study of $PKP(BC) - PKP(DF)$ residuals [*Bréger et al.,* 1999]. Alternative models, combining D" and outer core structure, as were first considered by *Ritzwoller et al.* [1986] and *Widmer et al.* [1992], fit the mode data equally well, except for a single mode, ${}_3S_2$, and therefore deserve further attention.

Acknowledgments. We thank Ruedi Widmer, Miyaki Ishii and Guy Masters for helpful reviews. The work presented in this paper was partially supported through NSF/EAR Program Grant EAR-9902777. It is BSL contribution 00-07.

References

Anderson, D. L. and R. L. Kovach, Attenuation in the mantle and rigidity of the core from multiply reflected core phases, *Proc. Natl. Acad. Sci. U.S.A., 51*, 168-172, 1964.

Bolton, H. and G. Masters, A region of anomalous $d\ln V_s/d\ln V_p$ in the deep mantle, *Eos Trans. AGU, 77*(46), Fall Meet. Suppl., F697, 1996.

Braginsky, S. I., Structure of the F layer and reasons for convection in the Earth's core, *Sov. Phys. Dokl., 149*, 8-10, 1963.

Braginsky, S. I., MAC -Oscillations of the hidden ocean of the core, *J. Geomagn. Geoelectr, 45*, 1517-1538, 1993.

Bréger, L., and B. Romanowicz, Three-dimensional structure at the base of the mantle beneath the Central Pacific, *Science, 282*, 718-720, 1998.

Bréger, L., B. Romanowicz, and H. Tkalcic, $PKP(BC - DF)$ travel times residuals and short scale heterogeneity in the deep earth, *Geophys. Res. Lett.,26*, 3169-3172, 1999.

Bréger, L., H. Tkalcic, and B. Romanowicz, The effect of D" on $PKP(AB-DF)$ travel time residuals and implications for inner core structure, *Earth Planet. Sci. Lett.*, 75, 133-143, 2000.

Creager, K.C., Anisotropy of the inner core from differential travel times of the phases PKP and $PKIKP$, *Nature, 356*, 309-314, 1992.

Creager, K.C., Inner core rotation rate from small-scale heterogeneity and time-varying travel times, *Science, 278*, 1284-1288, 1997.

Creager, K.C., Large-scale variations in inner core anisotropy, *J. Geophys. Res., 104*, 23,127-23,139, 1999.

Durek, J., and B. Romanowicz, Inner core anisotropy inferred by direct inversion of normal mode spectra, In press *Geophys. J. Int.,139*, 599-622, 1999.

Dziewonski, A. M., and D.L. Anderson, Preliminary reference Earth model, *Phys. Earth Planet. Inter., 25*, 297-356, 1981.

Garnero, E. J., and D.V. Helmberger, On seismic resolution of lateral heterogeneity in the Earth's outermost core, *Phys. Earth Planet. Inter., 88*, 117-130, 1995.

Garnero, E. J., and D.V. Helmberger, Seismic detection of a thin laterally varying boundary layer at the base of the mantle beneath the central-Pacific, *Geophys. Res. Lett., 23*, 977-980, 1996.

Glatzmeier, G. A., and P. H. Roberts, A three-dimensional convective dynamo solution with rotating and finitely conducting inner core and mantle, *Phys. Earth Planet. Inter., 91*, 63-75, 1995.

Gwinn,C. R., T. A. Herring, and I.I. Shapiro, Geodesy by radio interferometry: Studies of the forced nutations of the Earth, 2 Interpretation, *J. Geophys. Res., 91*, 4755-4765, 1986.

He, X. and J. Tromp, Normal-mode constraints on the structure of the Earth, *J. Geophys. Res., 101*, 20,053-20,082, 1996.

Hollerbach, R., and C. A. Jones, On the magnetically stabilizing role of the Earth's inner core, *Phys. Earth Planet. Inter., 87*, 171-181, 1995.

Ishii, M., and J. Tromp, Normal-mode and free-air gravity constraints on lateral variations in velocity and density of Earth's mantle, *Science, 285*, 1231-1236, 1999.

Kohler, M., Three-dimensional velocity structure and resolution of the core-mantle boundary region from whole mantle inversions of body waves, *Phys. Earth Planet. Inter., 101*, 85-104, 1995.

Kuo, C., J. Durek, and B. Romanowicz, Mantle heterogene-

ity inferred from normal mode spectra, *Eos Trans. AGU*, *79*(45), Fall Meet. Suppl., F627, 1998.

Lay, T., and C. J. Young, The stably-stratified outermost core revisited, *Geophys. Res. Lett.*, *17*, 2001-2004, 1990.

Li, X. D., and B. Romanowicz, Global mantle shear velocity model developed using nonlinear asymptotic coupling theory, *J. Geophys. Res.*, *101*, 22,245-22,272, 1996.

Li, X. D., D. Giardini, and J. H. Woodhouse, Large-scale three-dimensional even-degree structure of the Earth from splitting of long-period normal modes, *J. Geophys. Res.*, *96*, 551-557, 1991.

Lister, J. R., and B. A. Buffett, Stratification of the outer core at the core-mantle boundary, *Phys. Earth Planet. Inter.*, *105*, 5-19, 1998.

Masters, G., and F. Gilbert, Structure of the inner core inferred from observations of its spheroidal shear modes, *Geophys. Res. Lett.*, *8*, 569-571, 1981.

Mochizuki, E., and T. Ohminato, On the anomalous splitting of Earth's free oscillations, *Geophys. Res. Lett.*, *16*, 1415-1416, 1989.

Morelli, A., A.M. Dziewonski, and J. H. Woodhouse, Anisotropy of the core inferred from PKIKP travel times, *Geophys. Res. Lett.*, *13*, 1545-1548, 1986.

Obayashii, M., and Y. Fukao, P and PcP travel time tomography for the core-mantle boundary, *J. Geophys. Res.*, *102*, 17,825-18,841, 1997.

Poirier, J. P., Light elements in the Earth's core: A critical review, *Phys. Earth Planet. Inter.*, *85*, 319-337, 1994.

Poupinet, G., R. Pillet, and A. Souriau, Possible heterogeneity of the Earth's core deduced from $PKIKP$ travel times, *Nature*, *305*, 204-206, 1983.

Resovsky, J. S., and M. H. Ritzwoller, New and refined constraints on 3-D Earth structure from normal modes below 3 mHz, *J. Geophys. Res.*, *103*, 783-810, 1998.

Resovsky, J. S., and M. H. Ritzwoller, Regularization uncertainty in density models estimated from normal mode data, *Geophys. Res. Lett.*,*26*, 2319-2322, 1999.

Ritsema, J., S. Ni, D.V. Helmberger, and H.P. Crotwell, Evidence for strong shear velocity reductions and velocity gradients in the lower mantle beneath Africa, *Geophys. Res. Lett.*, *25*, 4245-4247, 1998.

Ritzwoller, M., G. Masters, and F. Gilbert, Observations of anomalous splitting and their interpretation in terms of aspherical structure, *J. Geophys. Res.*, *91*, 10,203-10,228, 1986.

Robertson, G. S. and J. H. Woodhouse, Evidence for proportionality of P and S heterogeneity in the lower mantle, *Geophys. J. Int.*, *123*, 85-116, 1995.

Robertson, G. S., and J. H. Woodhouse, Ratio of relative S to P heterogeneity in the lower mantle, *J. Geophys. Res.*, *101*, 20,041-20,052, 1996.

Romanowicz, B., X.-D. Li, and J. Durek, Anisotropy in the inner core: Could it be due to low-order convection?, *Science*, *274*, 963-966, 1996.

Sato, R., and A. F. Espinosa, Dissipation in the Earth's mantle and rigidity and viscosity in the earth's core determined from waves multiply reflected from the mantle-core boundary, *Bull. Seismol. Soc. Am.*, *57*, 829-855, 1967.

Shearer, P.M., $PKP(BC)$ versus $PKP(DF)$ differential travel times and aspherical structure in the Earth's inner core, *J. Geophys. Res.*, *96*, 2233-2247, 1991.

Shearer, P.M., K.M. Toy, and J.A. Orcutt, Axi-symmetric Earth models and inner core anisotropy, *Nature*, *333*, 228-232, 1988.

Song, X.-D., Anisotropy in central part of inner core, *J. Geophys. Res.*, *101*, 16,089-16,097, 1996.

Song, X.-D. and D.V. Helmberger, Seismic evidence for an inner core transition zone, *Science*, *282*, 924-927, 1998.

Souriau, A., and G. Poupinet, A latitudinal pattern in the structure of the outermost liquid core, revealed by the travel times of $SKKS - SKS$ seismic phases, *Geophys. Res. Lett.*, *17*, 2005-2007, 1990.

Souriau, A. and G. Poupinet, A study of the outermost liquid core using differential travel times of the SKS, $SKKS$, and S_3KS phases, *Phys. Earth Planet. Inter.*, *68*, 183-199, 1991.

Stevenson, D. J., Limits on lateral density and velocity variations in the Earth's outer core, *Geophys. J. R. Astron. Soc.*, *88*, 311-319, 1987.

Stixrude, L., and R. Cohen, High-pressure elasticity of iron and anisotropy of Earth's inner core, *Science*, *275*, 1972-1975, 1995.

Su, W. and A.M. Dziewonski, Inner core anisotropy in three dimensions. *J. Geophys. Res.*, *100*, 9831-9852, 1995.

Su, W., and A.M. Dziewonski, Simultaneous inversion for 3-D variations in shear and bulk velocity in the mantle, *Phys. Earth Planet. Inter.*, *100*, 135-156, 1997.

Tanaka, S., and H. Hamaguchi, Degree one heterogeneity at the top of the Earth's core, revealed by $SmKS$ travel times, in *Dynamics of Earth s Deep Interior and Earth Rotation*, *Geophys. Monogr. Ser.*, vol. 72, edited by J. L. Le Mouel et al.,pp 127-134, AGU, Washington, D.C., 1993.

Tanaka, S., and H. Hamaguchi, Degree one heterogeneity and hemispherical variation of anisotropy in the inner core from PKP(BC)-PKP(DF) times, *J. Geophys. Res.*, *102*, 2925-2938, 1997.

Tromp, J., Support for anisotropy of the Earth's inner core from splitting in free oscillation data, *Nature*, *366*, 678-681, 1993.

Tromp, J., Normal-mode splitting observations from the great 1994 Bolivia and Kuril Islands earthquakes: Constraints on the structure of the mantle and inner core, *GSA Today*, *5*, 137-151, 1995.

Tromp, J., and E. Zanzerkia, Toroidal splitting observations from the great 1994 Bolivia and Kuril Islands earthquakes, *Geophys. Res. Lett.*, *22*, 2297-2300, 1995.

Vasco, D., and L. Johnson, Whole Earth structure estimated from seismic arrival times, *J. Geophys. Res.*, *103*, 2633-2672, 1998.

Vinnik, L., B. Romanowicz, and L. Bréger, Anisotropy in the center of the inner core, *Geophys. Res. Lett.*, *21*, 1671-1674, 1994.

Wahr, J., and D. de Vries, The possibility of lateral structure inside the core and its implications for nutation and Earth tide observations, *Geophys. J. Int.*, *99*, 511-519, 1989.

Widmer, R., G. Masters, and F. Gilbert, Observably split multiplets-data analysis and interpretation in terms of large-scale aspherical structure, *Geophys. J. Int.*, *111*, 559-576, 1992.

Woodhouse, J.H., D. Giardini, and X.-D. Li, Evidence for inner core anisotropy from splitting in free oscillation data, *Geophys. Res. Lett.*, *13*, 1549-1552, 1986.

Wysession, M. E., Large-scale structure at the core-mantle boundary from diffracted waves, *Nature*, *382*, 244-248, 1996.

B. Romanowicz and L. Bréger Seismological Laboratory, 207 McCOne Hall, Berkeley, CA 94720. (barbara@seismo.berkeley.edu, breger@seismo.berkeley.edu)

(Received May 27, 1999; revised April 7, 2000;
accepted April 13, 2000.)